DESIGN AND CHARACTERIZATION OF VARIABLE ACOUSTIC FIELD AMPLITUDE AND FOCUSING ULTRASONIC TRANSDUCERS

by

John W. Gray

Thesis submitted to the Faculty of the

Virginia Polytechnic Institute and State University

in partial fulfillment of the requirements for the degree of

MASTER OF SCIENCE

in

Electrical Engineering

APPROVED:

Dr. Richard O. Claus

Dr. Charles E. Nunnally

Dr. Leonard L. Grigsby

May, 1983
Blacksburg, Virginia

DESIGN AND CHARACTERIZATION OF VARIABLE ACOUSTIC FIELD AMPLITUDE AND FOCUSING ULTRASONIC TRANSDUCERS

by

John Walker Gray, III

(ABSTRACT)

Ultrasonic transducers with concentric annular ring electrodes can be used to generate various circularly symmetric acoustic field profiles. These transducers can also electronically simulate a circular phased array and generate a focused ultrasonic beam. A model which predicts the acoustic transducer output for a given scaled voltage input has been developed. Several transducers have been designed using this model. Special attention has been given to the unique case of the two-dimensional radially Gaussian amplitude profile. Fabrication techniques for these transducers have been developed and are discussed. A microprocessor-based data acquisition system is described which will characterize the two-dimensional transducer profile as well as the propagation profile along one radial axis. Example tests of some of these transducers are presented.

ACKNOWLEDGEMENTS

I thank my thesis advisor and friend, Dr. Richard O. Claus, for his advice, assistance, and the time he gave to help me get this thesis completed. I would also like to thank Dr. Charles Nunnally and Dr. Leonard Grigsby for serving as my graduate committee.

I would like to thank my fellow graduate students who began this work and inspired me to continue; Avinash Garg, Tyson Turner, Janet Wade, and Sam Zerwekh, and the undergraduates who assisted me this year, Mike Barsky, Randy Burrier, Steve Krafft, Bill O'Connor, and Ed Richter. I especially appreciate the time and advice of Dan Dockery who has been a great help. Vicki Trump, who has been invaluable in typing and correcting this manuscript while learning to hate the computer, deserves my special thanks.

Lastly, I would like to thank my family and friends for their support and patience and for listening to me wonder if I would ever be done.

TABLE OF CONTENTS

LIST OF FIGURES

Chapter I

INTRODUCTION

The applications of ultrasound have increased significantly since Langevin first used stacks of piezoelectric plates to produce the first practical hydrophone prior to World War I. Since then ultrasonic devices have been applied to biomedical tomography, ultrasonic electronic signal processing devices, ultrasonic material processing including cleaning, machining, welding, soldering, and atomization, and the nondestructive evaluation (NDE) of critical mechanical structures [1]. Each of these applications requires the use of a transducer to convert electrical input signals into ultrasonic output waves and the type of transducer required depends upon the specific application. In materials processing, for example, transducers are usually required which simply produce high amplitude ultrasonic fields. Control of both field amplitude and phase as functions of both space and time, however, is usually desirable for signal processing and material scanning systems. The objective of this work has been to consider methods for obtaining and measuring such field control.

1.1 MOTIVATION FOR GAUSSIAN AND FOCUSING TRANSDUCERS

1.1.1 Gaussian Profiles

Most ultrasonic transducers used for the generation and detection of bulk acoustic fields produce pulsed or time periodic pressure distributions which are nearly uniform across their active surface areas. Theoretical analyses have been conducted by several authors [2,3] into the advantages of using Gaussian profiled ultrasonic beams instead. For example, in measurements involving reflection and scattering, a field without sidelobes may be used to minimize ambiguities in reflector location. Thus, a convenient choice for the far field distribution, and so the transducer output field, is a Gaussian function of beam radius as illustrated in Figure 1.1. This is advantageous because the near and far field amplitude patterns are related by a two-dimensional Fourier transform, and the transform of a Gaussian function remains Gaussian.

1.1.2 Focusing Beams

Another analogy possible between electromagnetics and ultrasonics is the focusing of an ultrasonic beam in a manner similar to focusing an optical beam. This can be treated analytically using concepts similar to those used in phased array antenna theory [4]. Ultrasonic beam focusing is sometimes referred to by the term ultrasonic phasing for this reason. According to Meindl [3], focusing an ultrasonic beam has advantages and disadvantages. The motivation for obtaining a focused ultrasonic beam is usually to increase the lateral resolution of an imag-

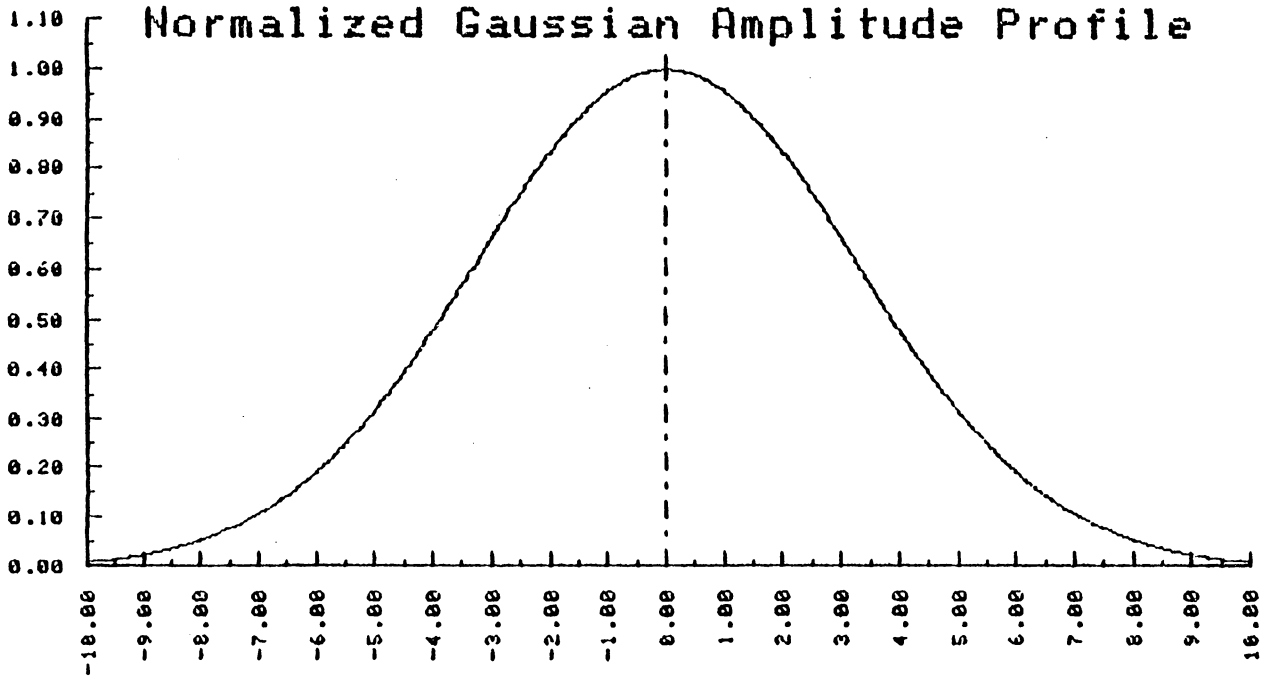

Figure 1.1: Gaussian Beam Profile

ing system. The resolution of unfocused systems is usually limited to the transducer diameter. Previous focusing applications have used curved solid or liquid lenses having fixed focal lengths to focus the beam to a spot in a plane located a fixed distance away from the transducer. The disadvantage of a focused beam is that the beam diverges rapidly beyond the back focal plane of the lens limiting all resolution to one fixed distance from the transducer. Dynamic focusing, using variable mechanical lenses, has been considered to be too difficult to implement for many applications.

Ultrasonic focusing can also be achieved electronically by feeding signals with different phases to the elements of a multi-electrode transducer. By combining the Gaussian profile and focusing transducer concepts, a valuable tool for ultrasonic imaging can be developed. Current research has developed both focusing and non-focusing Gaussian transducers which utilize identical transducer electrode designs. By combining the electronics for these two transducers, focusing two-dimensional Gaussian beams are possible. This is a description of work that both models these concepts analytically and characterizes transducers based upon the models.

1.2 ULTRASONIC TRANSDUCER BACKGROUND

1.2.1 Acoustic Waves

Before proceeding, a brief discussion of ultrasonic waves is useful. An ultrasonic wave is a sound wave with a frequency above the threshold of human hearing. The term acoustic is also often used interchangeably with the term ultrasonic although it does not imply such frequency constraints.

Acoustic waves are particle displacement or localized pressure fields which propagate in liquids, solids or gases. There are a variety of types of acoustical waves, with the two major ones in solids being transverse or shear waves and longitudinal waves. Particle displacement for a shear wave is perpendicular to the direction of propagation. One way to visualize this is as a wave propagating along a string, where the string motion is up and down and the wave travels from one end to the other. Longitudinal waves, on the other hand, are compressional in nature. With these, the direction of particle motion is parallel to the direction of propagation [5]. In this case, the propagation media can be thought of as a long spring and the wave as being started at one end by a quick push parallel to the axis of the spring. The resulting compressed region travels down the spring and the spring returns to its original position after the longitudinal wave passes.

1.2.2 Transducers

The transducers discussed here generate primarily longitudinal waves. The transducer element is a disk of quartz or other piezoelectric material. When a sinusoidal electric field is applied parallel to the circular axis of this disk, it mechanically expands and contracts along the axis. One technique to apply this electric field is to have metal deposited on both flat surfaces and to apply a voltage between these metal electrodes. When a high voltage of a given frequency is applied, the crystal will vibrate at that frequency, and ultrasound will be emitted. At certain frequencies which depend upon crystal thickness, a larger vibration will occur. These are the crystal's resonant mechanical frequencies. If only a voltage pulse rather than a continuous signal is applied to the crystal, the crystal will emit a short burst of ultrasound at the resonant frequency. Most of the experiments detailed later in this thesis were operated in the pulsed mode.

1.2.3 Transducer Acoustic Fields

In order to generate Gaussian profile and arbitrary-profile focusing ultrasonic fields, the uniformly electroded transducer can be modified in several ways. As indicated above, this can be done either by modifying the field after it is emitted from the transducer or by modifying the transducer itself. Most prior focusing work has involved the use of external lenses while prior Gaussian profile approximations have been obtained using various single electrode geometries. As part of recent

research, a transducer electrode geometry has been designed which is capable of generating both focusing and Gaussian ultrasonic beams. Unlike other designs which utilize single electrode field fringing effects or star pattern geometries to produce an averaged Gaussian profile [6, 7], this transducer uses circularly symmetric ring electrodes driven with amplitude-weighted voltages selected to form an optimized approximation to a Gaussian function. When these ring electrodes are driven appropriately out-of-phase, or have variable delay pulses applied, a focusing beam is generated.

1.2.4 Transducer Research

The direction of this research has been four-fold. The first problem has been to develop and refine the theory of ring transducers. Previous work in the area of Gaussian ring transducers assumed a linear variation of electric field between adjacent rings [8]. Narrow electrodes however, display significant fringing effects [7], and a better model of field variation is needed. Such a model has been developed which provides a higher order approximation to the field emitted by a voltage weighted ring transducer. This allows more accurate computer-aided design of the ring dimensions and voltage weighting functions. Refinements also have been made to another computer model which calculates the timing delays for a focusing ring transducer to implement a more general transducer design. These topics are discussed in Chapter 2.

1.2.5 Fabrication

Once these design models are used, the designed transducer must be fabricated. Due to the multi-ring, multi-connector problem with these transducers, techniques were needed that would provide a water tight seal around the transducer as well as acoustically load the back of the transducer. The fabrication techniques developed with the aid of a student in materials engineering [9] are presented in Chapter 3.

1.2.6 Testing System

The third phase of the project has been to develop and build a comprehensive transducer testing system. Previous research projects had constructed a water tank and a portion of a computer system but many elements of the system were incomplete. My work in this area has been to redesign and implement the existing elements into a complete transducer testing and characterization system to evaluate the transducers designed above. This system has been designed to be reliable, flexible, and ergonomically sound. Both the hardware and software of this system are described in Chapter 4.

The final aspect of the research has been to design, construct, and test various Gaussian and focusing transducers. For several of these designs, scanned acoustic field results are presented in Chapter 5. The primary research effort, however, has been to create a system used for the design, construction, and analysis of these types of transducers rather than to experimentally measure the fields shown in these scans.

Chapter II

TRANSDUCER THEORY

The concepts of the radially symmetric Gaussian profile and of a focused ring transducer can be handled separately and then combined in order to generate the focused Gaussian. The technique used to generate the Gaussian profile is to change the voltage amplitude applied to each ring. When focusing a transducer, either the phase of a cw rf signal is adjusted between each ring or a time delay is inserted on each pulse for a given ring. This phase or delay is calculated for each ring to properly phase the ultrasonic waves at the focal plane. Because neither one of these techniques has any dependency on the other, they may be done simultaneously to obtain the focused Gaussian. Typical applications of such profiled ultrasonic fields are in biomedical ultrasound imaging systems, the non-destructive evaluation of materials, and the generation of the Schoch effect beam shift at solid-liquid interfaces [10]. The Schoch effect is difficult to solve analytically when sidelobes are present in the input beam but may be solved if they are not. In the biomedical and NDE applications, the ultrasonic beam is propagated through a specimen which may contain a defect. In order to reconstruct an image of the defect, the profiles both of the incident and received ultrasonic fields need to be known. For uniform profile transducers, the above constrains the defect to be either in the very near field or very far field of the transducer. At other distances the field is difficult to characterize without knowledge of the exact distance.

2.1 GAUSSIAN BEAM PROPAGATION

As an acoustic beam propagates, it is affected by the medium it is propagating through. Because of adjacent particle mechanical strains and due to the beam interfering with itself, the shape of the beam changes. In general, the beam will both diverge, that is become wider, and different from its original amplitude profile. In the far field case, the ultrasonic beam amplitude profile will have become the Fourier transform of the input amplitude profile. For example, a true uniform input transducer profile will transform into the

$$\frac{\sin(x)}{x}$$

function in the far field [4]. A Gaussian beam, however, remains Gaussian at all points along its propagation path in a homogeneous medium. Upon reaching a discontinuity, a Gaussian beam profile changes due to reflection and scattering. It is easier to obtain information about a defect in a Gaussian ultrasonic beam because the field profile at the location of the defect is a simple Gaussian function [2]. For these reasons, a Gaussian profile transducer would be a useful device.

2.2 THEORY OF GAUSSIAN PROFILE RING TRANSDUCER

A two-dimensional Gaussian surface exhibits the property of radial symmetry, allowing analyses to proceed in one dimension. The normalized Gaussian function in polar coordinates may be expressed as

$$G(\rho,\theta) = e^{-(\rho^2)/(2\sigma^2)}, \qquad \text{for all } \theta, \tag{2.1}$$

where θ is the standard deviation of the function. A Gaussian profile cross section was shown in Figure 1.1.

A transducer geometry which exhibits radial symmetry is a set of rings which are concentric about the center of the transducer, illustrated in Figure 2.1. If each ring has an appropriately scaled voltage applied, radially symmetric electric and stress fields will be generated in the crystal and the generated acoustic field will maintain radial symmetry. All that needs be done to generate a desired field shape, therefore, is to calculate the proper voltage for each ring. Previous work with Gaussian profiled fields has been based upon a linear approximation for the field between adjacent rings and the assumption that no interaction occurs between rings. The resulting model led to the operation of a viable Gaussian transducer [8]. The model approximations are coarse, however, and may be improved.

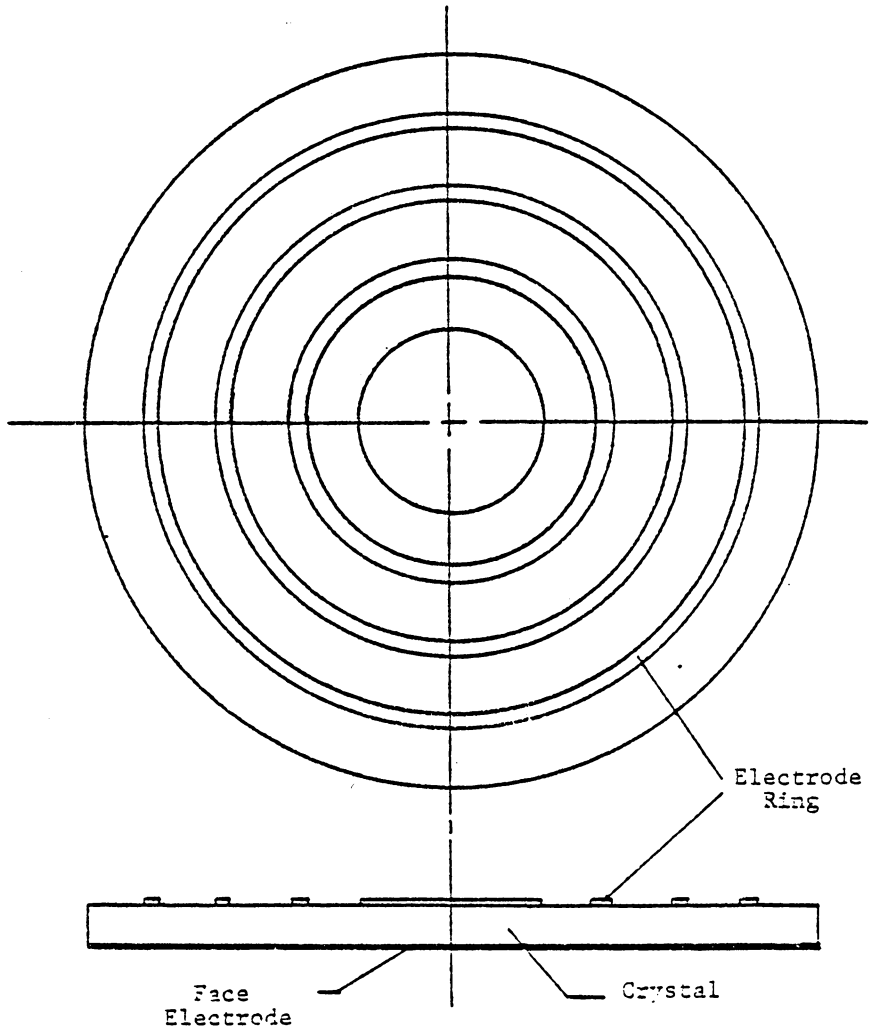

Figure 2.1: Concentric Ring Transducer Element

2.2.1 Higher Order Approximation

The principle of the higher order approximation is that the fringing of each ring contributes to the acoustic field at the points on the transducer face and the total field may be found by summing the individual ring fields. Because many piezoelectric crystals have a linear response with respect to applied voltage, the effect of each ring may be scaled by the relative voltage applied.

2.2.2 Ideal Approach

The ideal approach to the field calculation would be to solve for the mechanical stress at each point on the ρ axis at the face of the transducer by a double integration. The first integration would be around each ring for $0 \leq \theta \leq 2\pi$ and would evaluate the electric field as a function of radius and position between the two surfaces of the crystal. Then the scaled contributions of all rings would be summed and a second integration would be made from one face to another. In converting electric field properties to mechanical vibration amplitudes, this integration, however, would have to take into account the relative effects of:

1. distance from the transducer front surface to the total mechanical vibration and
2. mechanical loading on the crystal back.

Since these effects have not been measured, and due to the large number of analytical integrations required, this approach is impractical.

2.2.3 Partial Electrode Approximation

There is clearly a need for a theoretical approach which lies between these two extremes. A strong beginning point has been provided by Breazeale and Martin [11]. They analyze the case of a simple strip electrode and present an equation for the electric field at the face of the transducer. They then claim that this approximates to a reasonable degree the acoustic field generated at the transducer face. This approximation is then substantiated with experimental results. The formula they use to derive the electric field is:

$$E_z(x) = \frac{Q(t)\ b}{2a} \int_{x_s=-a}^{a} \frac{dx_s}{u^2(u^2+c^2)^{\frac{1}{2}}}, \tag{2.2}$$

where:

$Q(t)$ = charge on electrode,

$u = (x-x_s)^2+b^2$,

a = electrode width,

b = crystal thickness,

c = electrode length,

Integrating along the x axis yields

$$E_z(x) = \frac{Q(t)}{2a}\left[\sin^{-1}\left(\frac{c(a-x)}{(b^2+c^2)^{\frac{1}{2}}[(a-x)^2+b^2]^{\frac{1}{2}}}\right) + \sin^{-1}\left(\frac{c(a+x)}{(b^2+c^2)^{\frac{1}{2}}[(a+x)^2+b^2]^{\frac{1}{2}}}\right)\right]. \tag{2.3}$$

For the case of an electrode much longer than the crystal thickness, ($c >> b$),

this reduces to a summation of two angles

$$E_z(x) = \frac{Q(t)}{ac} (\alpha+\beta) \qquad (2.4)$$

where α and β are illustrated in Figure (2.2). The term

$$\frac{Q(t)}{ac},$$

represents the scaled voltage that has been applied to the electrode.

2.2.4 Adaptation to Circular Rings

Both Equations 2.3 and 2.4 above may be used to form an approximation to a circular electrode geometry. For the case of a ring on a thin crystal, the approximate formula has been used. This means that a circular electrode is being modeled as an infinite strip. Although there are several ways to apply the exact formula they require complicated integrations. Error is introduced in two ways:

1. by the curvature of the electrode instead of infinite strip, and
2. due to the curvature, the electrode may not be much "longer" than the crystal thickness.

These effects are more significant for smaller radius rings than for larger radius rings. The approximations thus made are shown graphically in Figure 2.3.

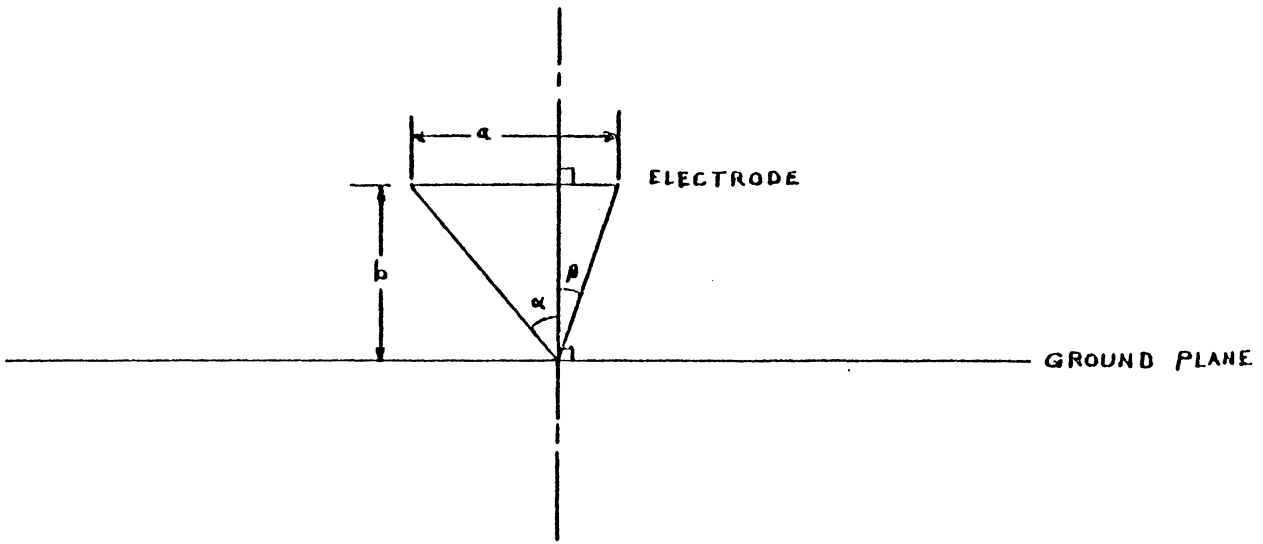

Figure 2.2: Strip Electrode Geometry

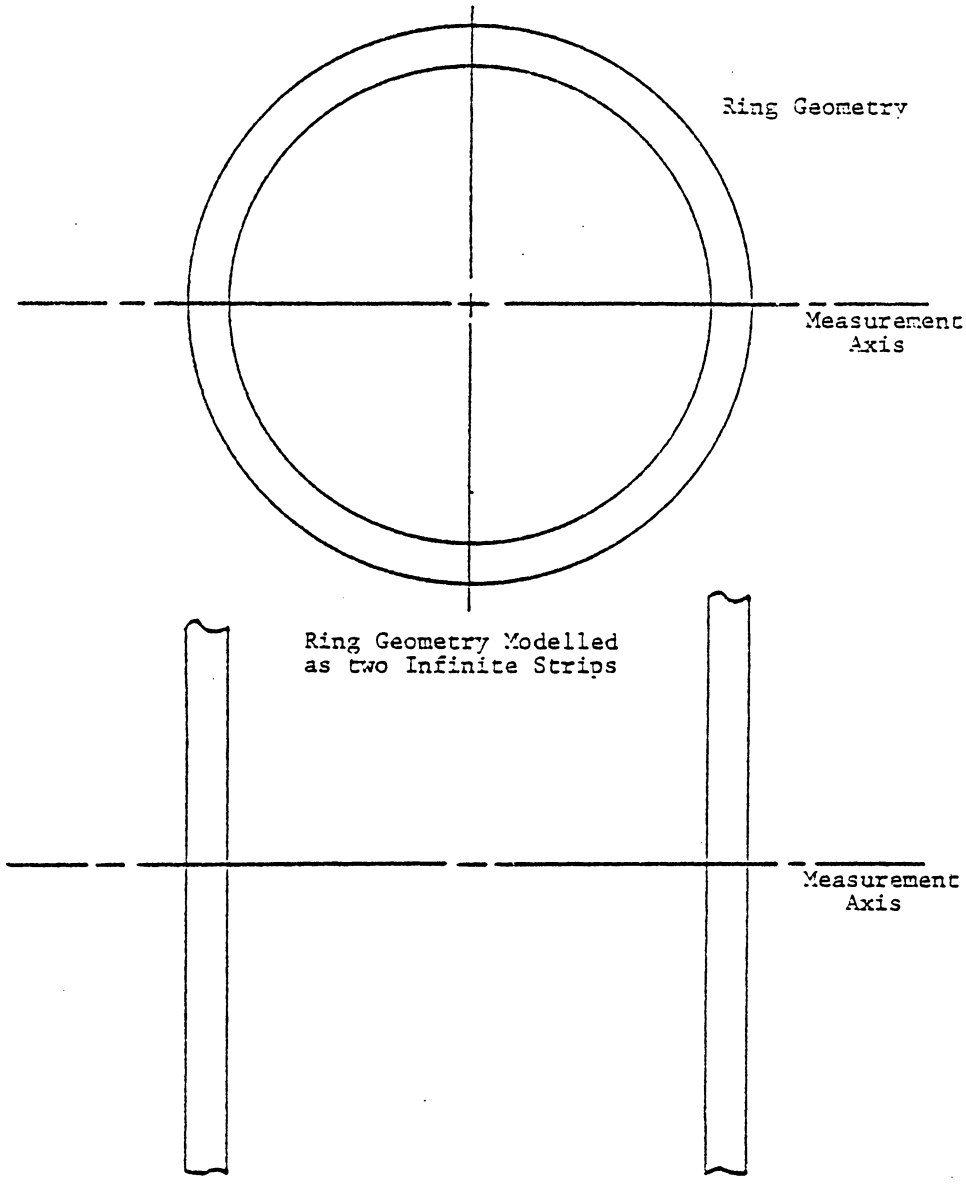

Figure 2.3: Ring Approximation

An analysis of the error due to the use of the approximation where the effective length may be short shows that for a length over width ratio of only five, the error between the exact formula and the angle approximation is less than two percent.

2.2.5 Special Case: Center Spot

Because the center electrode is a solid circle and not a ring, a different technique must be used. Use of Equation 2.4, the angle equation, would simulate a strip electrode of the same width as the center spot diameter and infinite length. As our case is for a finite length, however, it seems the exact equation, Equation 2.3, might be used. This would approximate the acoustic field of a circular electrode with that of a square, probably not a bad approximation. However, this case can be expanded to even more closely approximate the circle by using several rectangles to fill the circle and solving for the field generated by these using superposition. Five rectangles, Figure 2.4, seem to closely approximate the circle, a number chosen by graphical judgement. Of course, an infinite number of differentially wide rectangles would be an exact integration, but this would be very slow computationally.

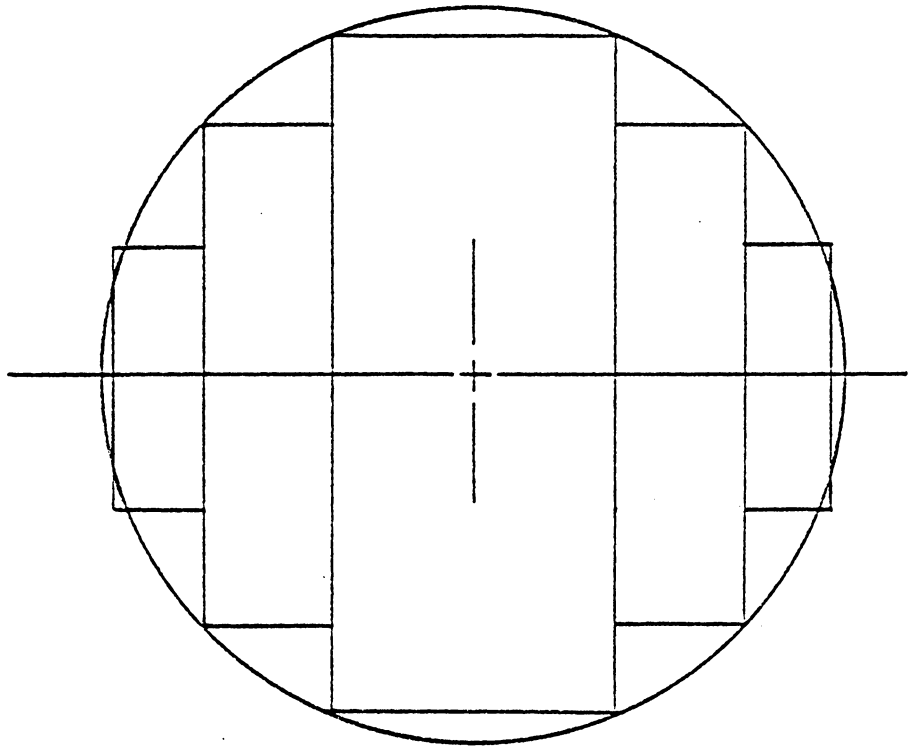

Figure 2.4: Center Spot Approximation

2.2.6 Acoustic Efficiency

An interesting result of the partially electroded transducer theory was observed. If a strip electrode is very narrow, it is evident that the sum of two small angles will also be small. Conversely, a very wide electrode would have two very large angles and would yield a large sum. The ultimate case would be an infinitely wide electrode, yielding a sum of π. Because of the linear relationship between this sum and the acoustic field, it is evident that a wider electrode produces a stronger peak acoustic amplitude. The maximum achievable amplitude would be for the infinite case. Using this one can define an acoustic efficiency as:

$$\text{efficiency} = \frac{\text{peak amplitude under electrode}}{\text{infinite electrode amplitude}} \times 100 \qquad (2.5a)$$

$$= \frac{E_z(x)}{\pi} \times 100, \qquad (2.5b)$$

where the infinite case amplitude yields π and the amplitude under the electrode is calculated using the equations above.

2.2.7 Aspect Ratio

Another feature that affects ring electrode design is the aspect ratio of the acoustic field generated by an electrode. An electrode which produces a peak field value that drops off rapidly before the next electrode will cause the output field to vary rapidly around the desired

function. Wide electrodes tend to have a much higher center amplitude versus edge amplitude than narrow electrodes. This is undesirable when fitting an acoustic field to a slowly varying function such as a Gaussian profile.

A tradeoff therefore exists between acoustic efficiency and smoothness of the transducer output. This is illustrated by the two cases shown in Figure 2.5, which has a narrow and a wide strip electrode. The wide electrode has a greater acoustic efficiency but has dropped off faster at the electrode edge. Both electrodes are shown of equal width on different horizontal scales to illustrate this feature. An interesting result of these ring width characteristics is that sometimes narrow rings may be at higher potentials than a much wider center spot to match acoustic field intensities into a smooth Gaussian. This will be seen in some of the experimental cases discussed later.

2.2.8 Empirical Justification

Although a large number of approximations have been used in the derivation of this transducer field model, I believe the results are still valid. As mentioned above, an exact solution is very difficult and involves a great many factors not easily determined. The original technique for the partially electroded case had its basis in empirical observations of the field produced by a strip electrode. Extension of this case to annular ring case provided predictions which have been experimentally validated, as shown in Figures 2.6a,b,c. These figures show data

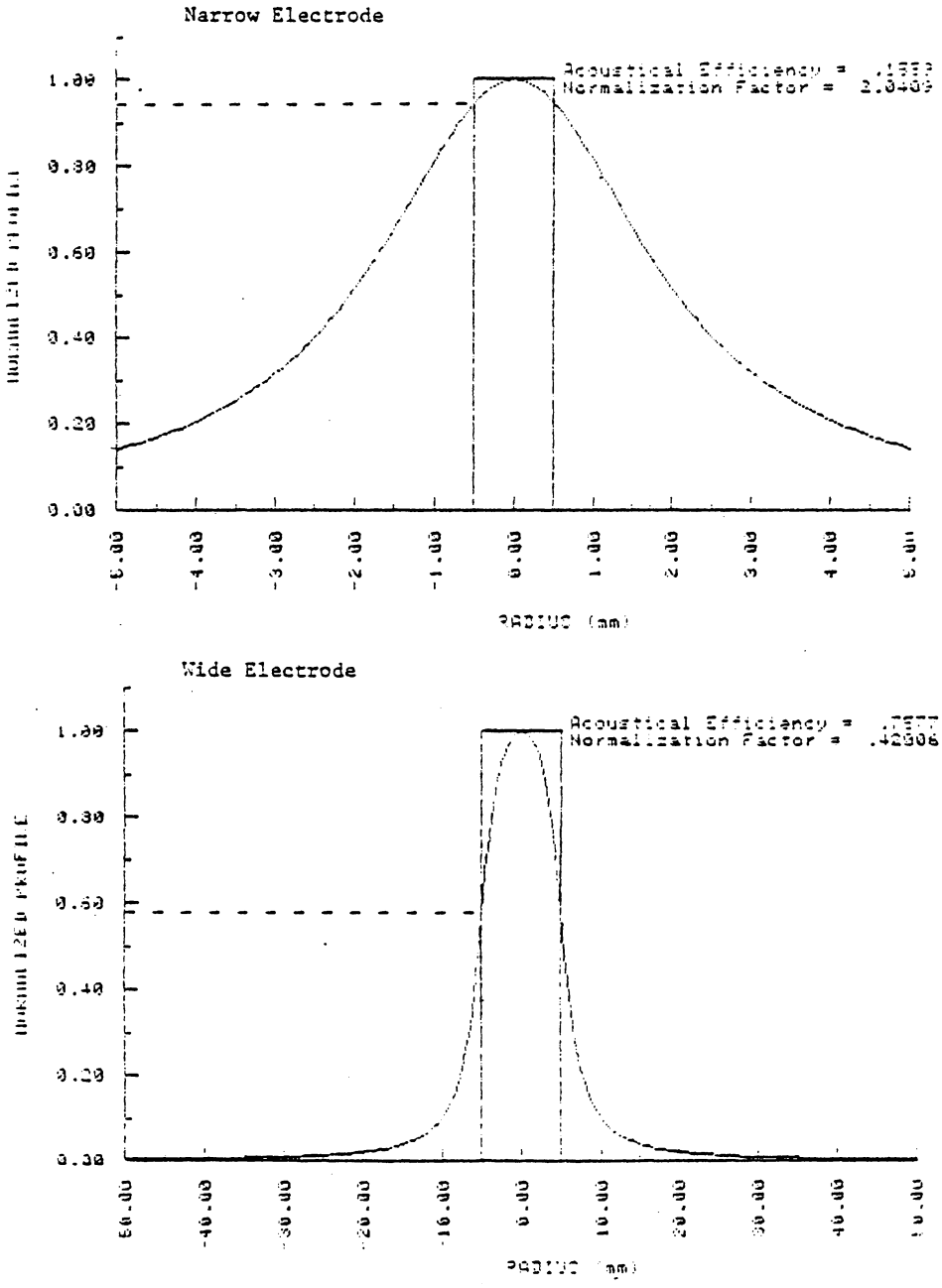

Figure 2.5: Aspect Ratio

of individual rings being pulsed compared to the predicted output for a ring at that location. The data and the prediction for each ring are normalized independently. The agreement of the data with the predicted output is very good for this approximation. Thus, although the derivation above is far from rigorous, it appears that the final approximation remains reasonably accurate and of higher order than a linear approximation.

2.2.9 RATOM: Ring Acoustic Transducer Output Model

Combining these approximations, it is possible to create an algorithm which can predict the acoustic output of a ring electrode piezoelectric transducer. By utilizing each of the equations above in the proper sequence and summing the results, the approximate acoustic output at any radial point on the transducer may be calculated. This algorithm, RATOM, uses the strip electrode approximation, Equation 2.4, for each ring and the five rectangle center spot approximation for the central disk electrode. A common notation has been adopted with this model to refer to the center spot and rings. The center spot, although not truly a ring, is notated as Ring 0, with a radius of R_0. Each ring beginning with the centermost ring, Ring 1, of radius R_1, is then numbered sequentially. The outer ring thus has the highest number, which is one less than the total number of electrodes on the transducer rear face.

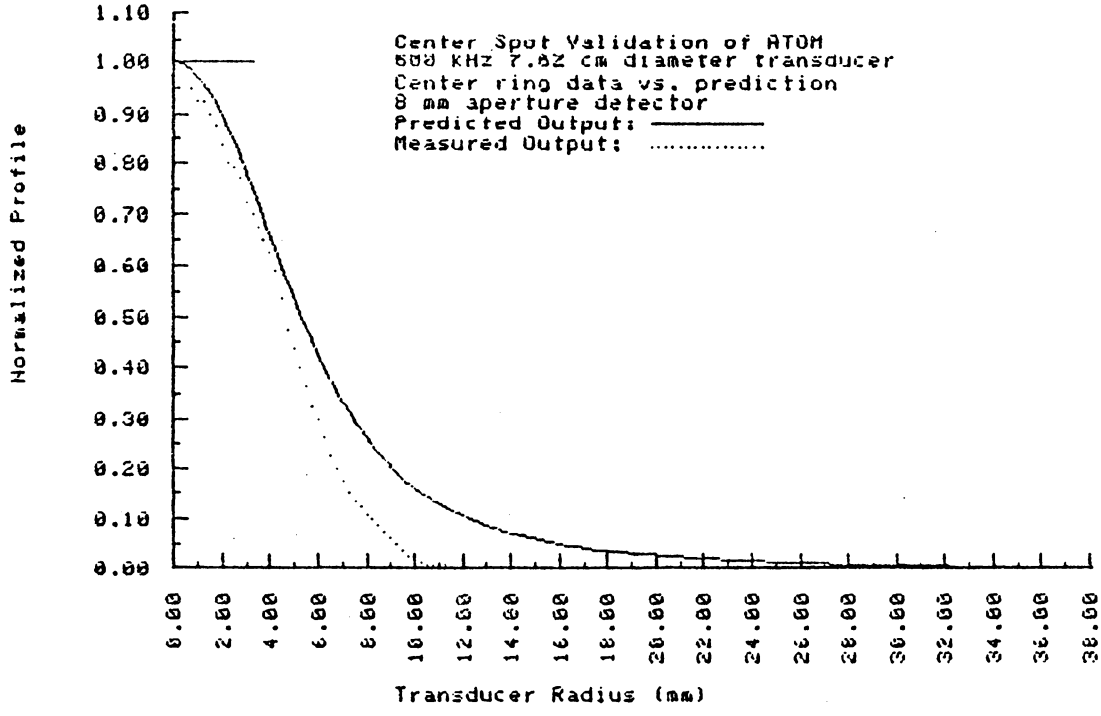

Figure 2.6a: Experimental Validation: Centerspot

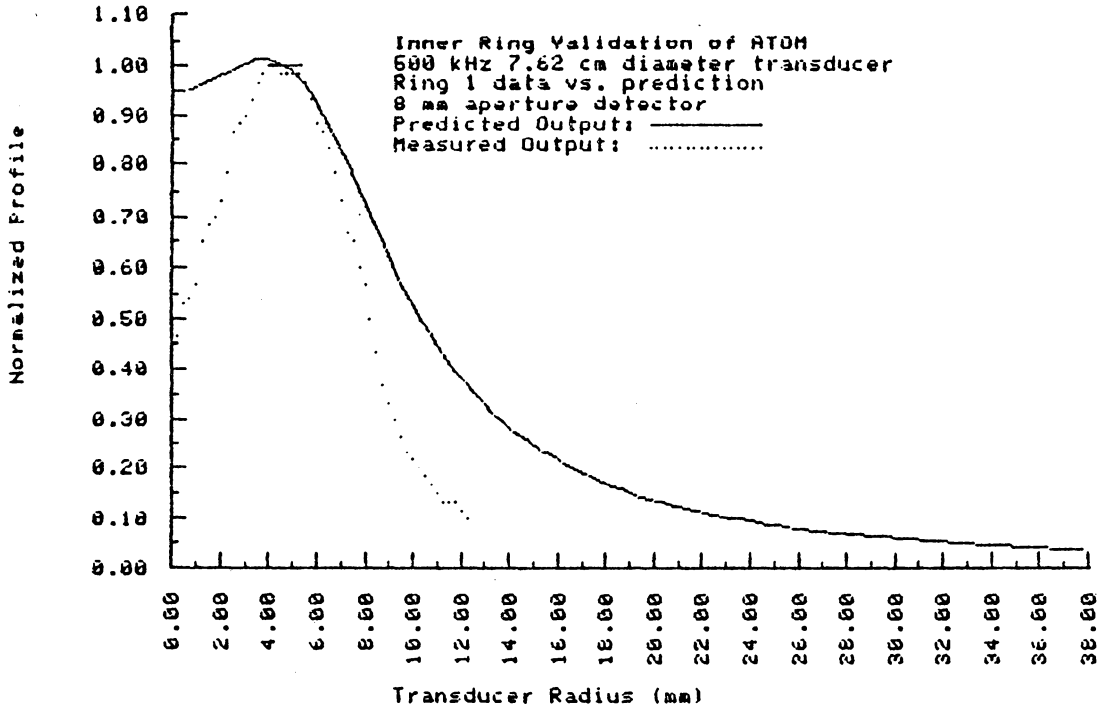

Figure 2.6b: Experimental Validation: Ring 1

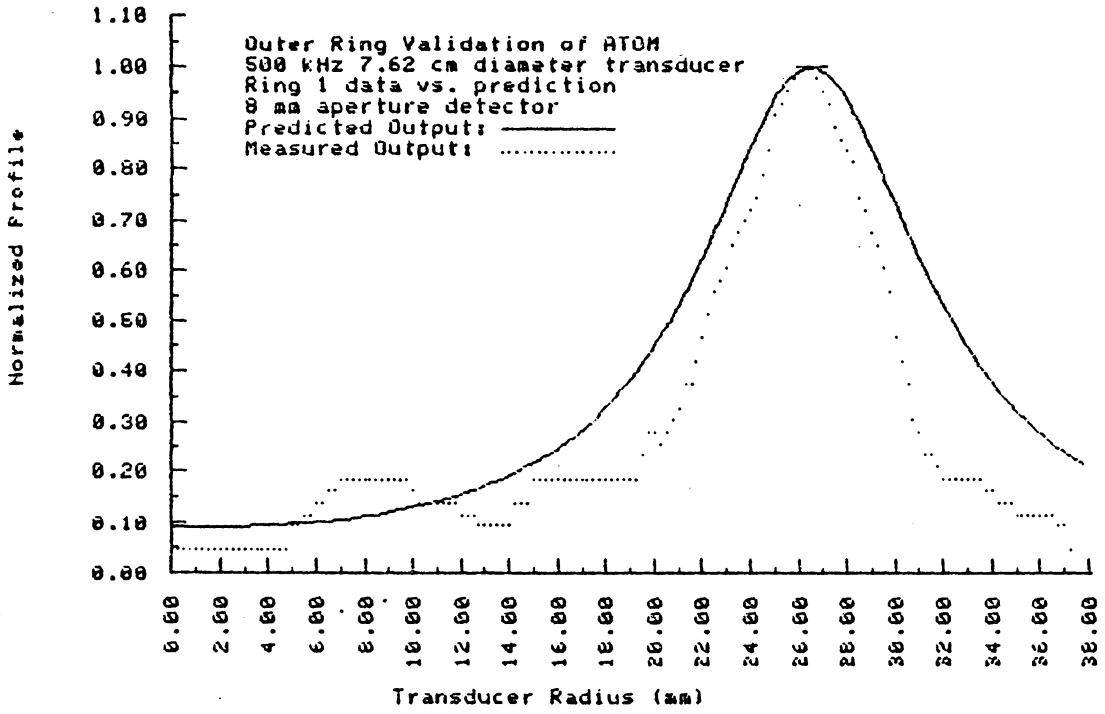

Figure 2.6c: Experimental Validation: Ring 10

2.2.10 Implementation of RATOM

Due to the large number of calculations required to solve for the predicted acoustic field over the diameter of the transducer, a simple computer program has been developed. This program uses the strip electrode approximation, Equation 2.4, for each ring and the five rectangle centerspot approximation for the central disk electrode. A plot is made using three parameters. First, the ideal function desired is plotted using a dotted line. Next, the predicted output is plotted on the same graph for comparison, using a solid line. The last parameter, the absolute error between these two, is plotted as a means of providing feedback as to the accuracy of the fit. This feedback allows the program user to adjust various parameters in an effort to try to decrease fit error.

For simplicity, the plot is made only along one radial of the transducer, from the center axis to the edge of the crystal. Other information is also contained in these graphs. The ring widths are plotted, with the vertical axis for the ring height representing relative potentials applied. The ring potentials may be either arbitrarily chosen by the user or chosen by a fit to a system of linear equations. All values are normalized to unity amplitude at the center of the transducer. Finally, exact ring radii, ring voltages, and other transducer variables are printed on the graph for identification. The program was written in BASIC for the HP 2647 graphics work station, and a listing is contained in Appendix (A.1). As much modularity as possible was used in

creating the program. The program also contains a simple Gaussian elimination technique for solving the system of linear equations for the ring potentials.

2.2.10.1 System of Linear Equations

If the desired acoustic output, the ring widths, and the ring radii are all known, it is possible to write a set of linear equations to solve for the individual ring voltages. The amplitude of the output acoustic energy at a specific point on the radius is a linear combination of the contributions from each ring to that point. The contribution of each ring is a function of the angles α and β scaled by the voltage applied to that ring. By requiring each acoustic output fixed value, f_n, to fall directly under the center of a ring, the exact voltages of all the other rings can be determined to fit the desired curve. This equation can be written in the form:

$$(\alpha_{00}+\beta_{00})V_0 + (\bar{\alpha}_{01}+\bar{\beta}_{01} + \overset{+}{\alpha}_{01}+\overset{+}{\beta}_{01})V_1 +\ldots+ (\alpha'_{0_n}+\beta'_{0_n})V_n = f_0$$

where:

$\alpha_{00}+\beta_{00}$ is the angle summation for the center spot,

V_0 is the center spot voltage,

$\bar{\alpha}_{01}+\bar{\beta}_{01}$ is the angle summation for the contribution of the first ring on the left side of the center,

$\overset{+}{\alpha}_{01}+\overset{+}{\beta}_{01}$ is the angle summation for the contribution of the first ring on the right side of the center,

V_1 is the voltage on the first ring,

$\alpha'_{0_n}+\beta'_{0_n}$ is the total angle summation for the contribution of the n-th ring,

V_n is the voltage on the outer ring,

f_0 is the desired field amplitude at the center spot.

This equation was written for the field at the center spot. A series of these equations can be written for each f_i at radius R_i. Because the α's and β's can be calculated geometrically, these are constants. The voltages V_i are the unknown quantity. Thus, this system is of the classical matrix form:

$$Ax = b \qquad (2.7)$$

and may be solved using any of the conventional techniques. Numerically, the solution is very nice because of the geometry of the problem. Each main diagonal element is usually the dominant element in that row. This means that a simple Gaussian elimination routine without pivoting will solve this problem without significant roundoff error. Such a routine was used as part of the computer model to solve for the voltages when the desired output field function was known.

2.2.11 Example Transducer Profiles Using RATOM

Once the program was created, many possibilities for profile shapes became apparent. The initial purpose of the program, however, was to generate electrode patterns and voltages for two transducer sizes specified by a development grant. This project involved creating both a

70.7 mm diameter and a 25.4 mm diameter 1 MHz Gaussian profile transducer pattern, and constructing the transducers. In both of these designs, great advantage was taken of the natural profile of the center spot to approximate the center of the Gaussian and rings to fill in at the edges. The 70.7 mm transducer required a center spot of radius 6.5 mm and five additional rings. The graphical output is shown as Figure 2.7. Note that the first ring is at a potential 1.4 times greater than the center spot, a feature due to the large variance in peak amplitude between a wide electrode and a narrow one. The second Gaussian was on the 25.4 mm crystal and was accomplished using only the center spot and one additional ring (Figure 2.8). Observe here that the error is non-zero immediately beneath the ring but has two zero error points on either side of the ring as well as under the center spot. This is due to user judgement rather than the linear fit program and resulted in a somewhat simpler design.

The next application of the program was to a thirteen electrode transducer previously designed for phasing experiments. Due to the nature of the electric field fringing of the inner electrodes, the outer ones were not required to form the Gaussian. This transducer was fabricated with an external input cable for each electrode to allow different experiments to be performed; more about the design will be discussed in Chapter 3 concerning transducer fabrication. This predicted profile is presented in Figure 2.9.

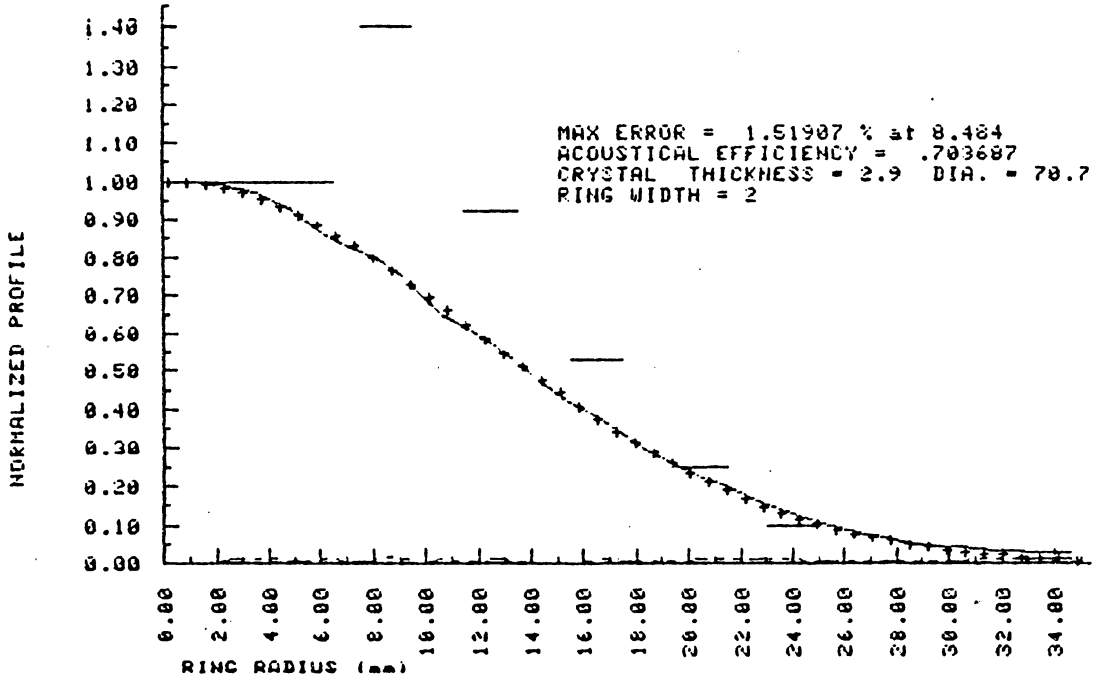

Figure 2.7: Ring Design: 70.7 mm, 1 MHz

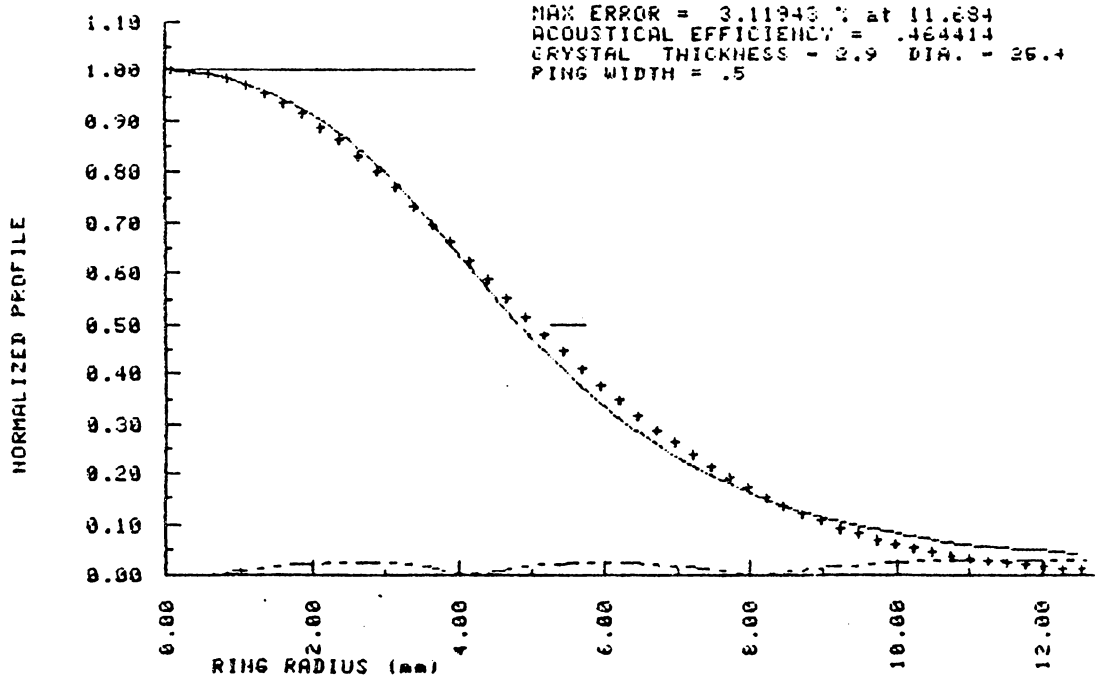

Figure 2.8: Ring Design: 25.4 mm, 1 MHz

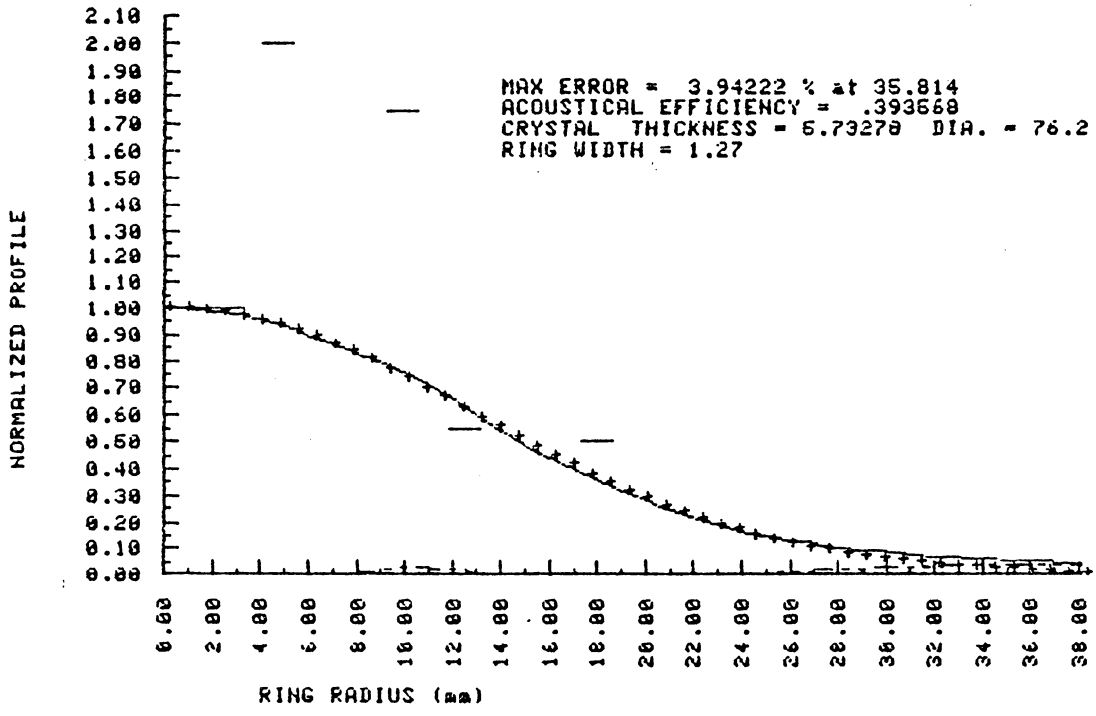

Figure 2.9: 500 kHz Gaussian Ring Voltages

RATOM is not merely limited to Gaussian profiles, however. Using just the center spot approximation on a uniformly electroded transducer produces the "uniform" profile of Figure 2.10. It is very interesting to note how much curvature the predicted function contains near the edges, radically differing from the cylinder or piston function usually assumed as the output for such a transducer. Immediate reflection on this result, however, indicates that potentially a concentric ring transducer such as used for the Gaussian function could be used to generate a "piston" profile, shown in Figure 2.11. The sharp discontinuity is achieved not because the electric field decays rapidly, but because a uniform field has been maintained up to the edge of the crystal, and there is no acoustic output beyond the edge of the piezoelectric crystal.

Various other transducer profiles have been predicted using this program. One case of interest here is the original Gaussian transducer profile developed by P. S. Zerwekh [8] using a linear model. By fortuitous choice of electrode widths and radii, his transducer exhibited a reasonably good fit to a Gaussian function, Figure 2.12, a fact validated by his data.

In conclusion, a relatively simple computative model for predicting transducer profiles has been presented. The algorithm is based on empirical observations and has been similarly validated. Several examples have been presented that were generated by a computer program of the algorithm. Although the algorithm is by no means exact or rigorous, it works well enough for experimental use.

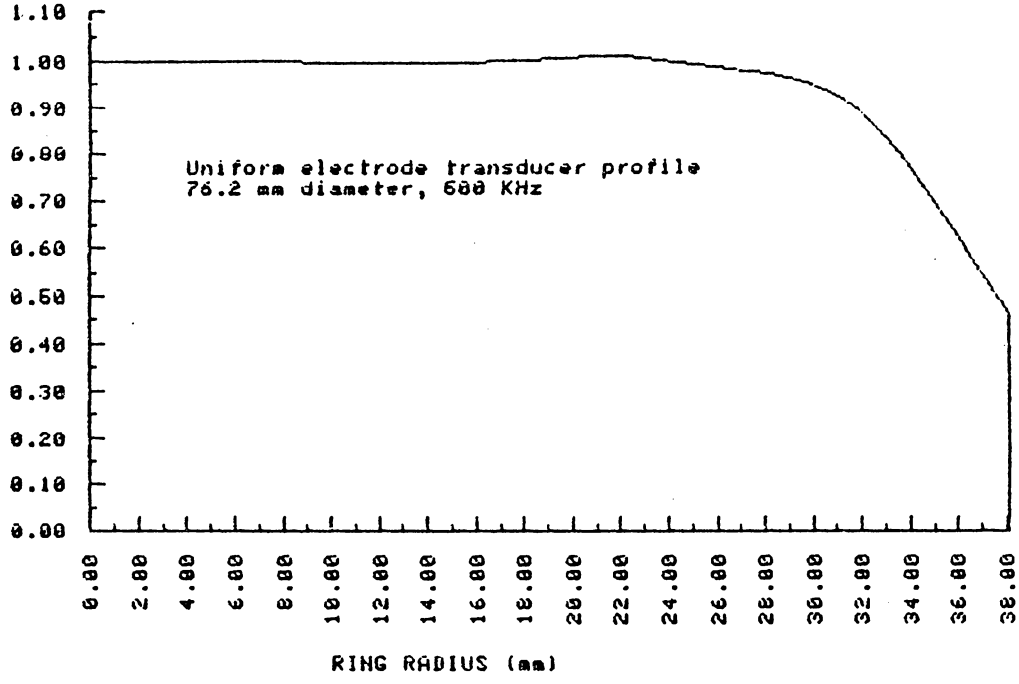

Figure 2.10: Uniform Electrode Transducer Profile

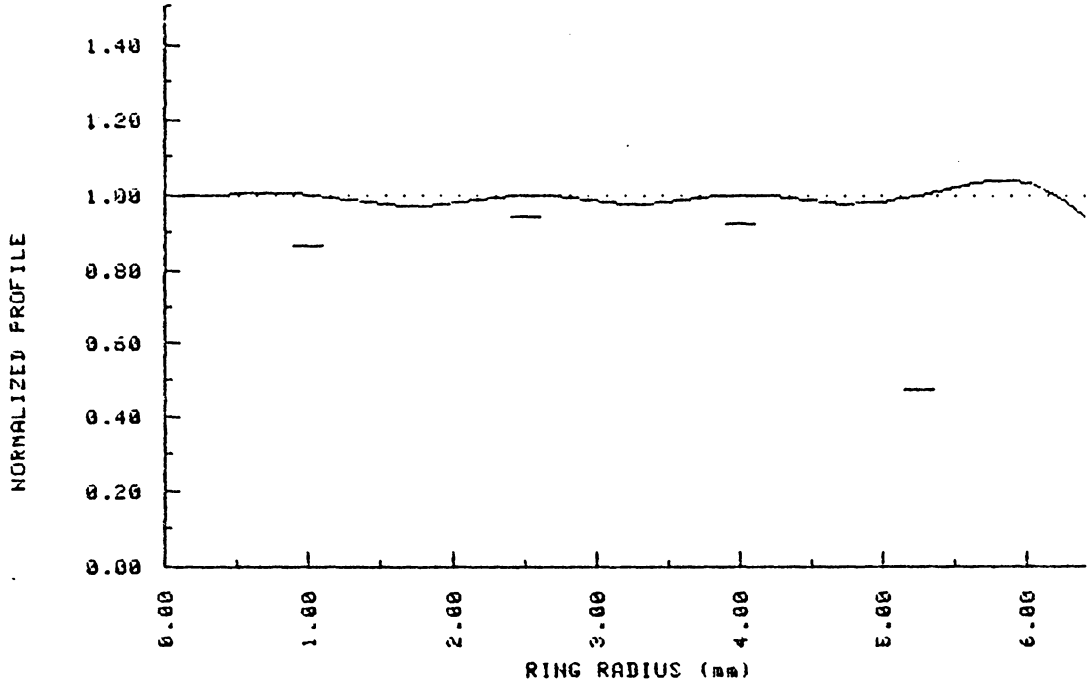

Figure 2.11: Ring Design: Piston Profile

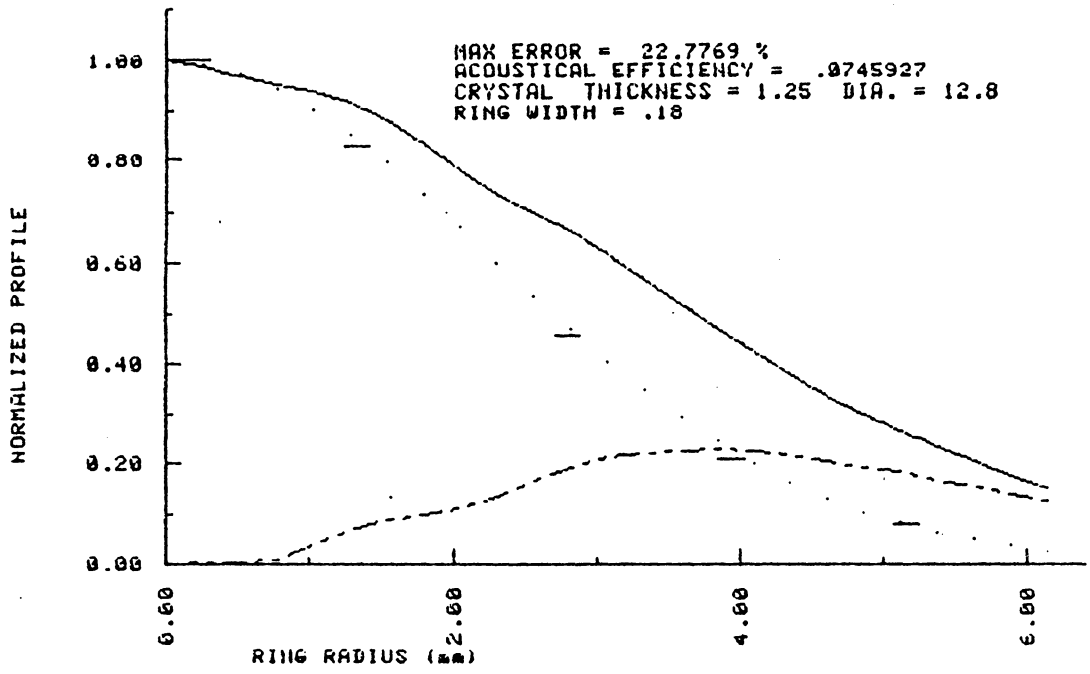

Figure 2.12: Original Gaussian Transducer Output

2.3 RING TRANSDUCER FOCUSING

The ring transducer geometry in one dimension can be modelled as an independent ultrasonic transducer array. All effects created by the array can be rotated to two dimensions in the same manner as a two-dimensional Gaussian is created from the one-dimensional case. The primary effect desired is the concentration of acoustic energy in a small region some distance from the face of the transducer array. This is known as ultrasonic beam focusing. For the pulsed ultrasonic array, Hildebrand [12] has developed a series of equations which model this focusing effect. Hildebrand's model is a geometric model using spherical acoustic wavefronts combining to constructively and destructively interfere. For the specific case of a ring transducer, at present only on-axis focusing is possible. The geometry for this case is shown in Figure 2.13. The time taken for the acoustic pulse to travel from the center source to the focal point along L_0 is the basic propagation time. Because L_1 is longer than L_0, the propagation time:

$$\text{prop. time(sec)} = \frac{\text{distance (cm)}}{\text{speed(cm/sec)}}$$

increases by an amount equal to

$$\text{delay} = \frac{L_1 - L_0}{\text{speed}},$$

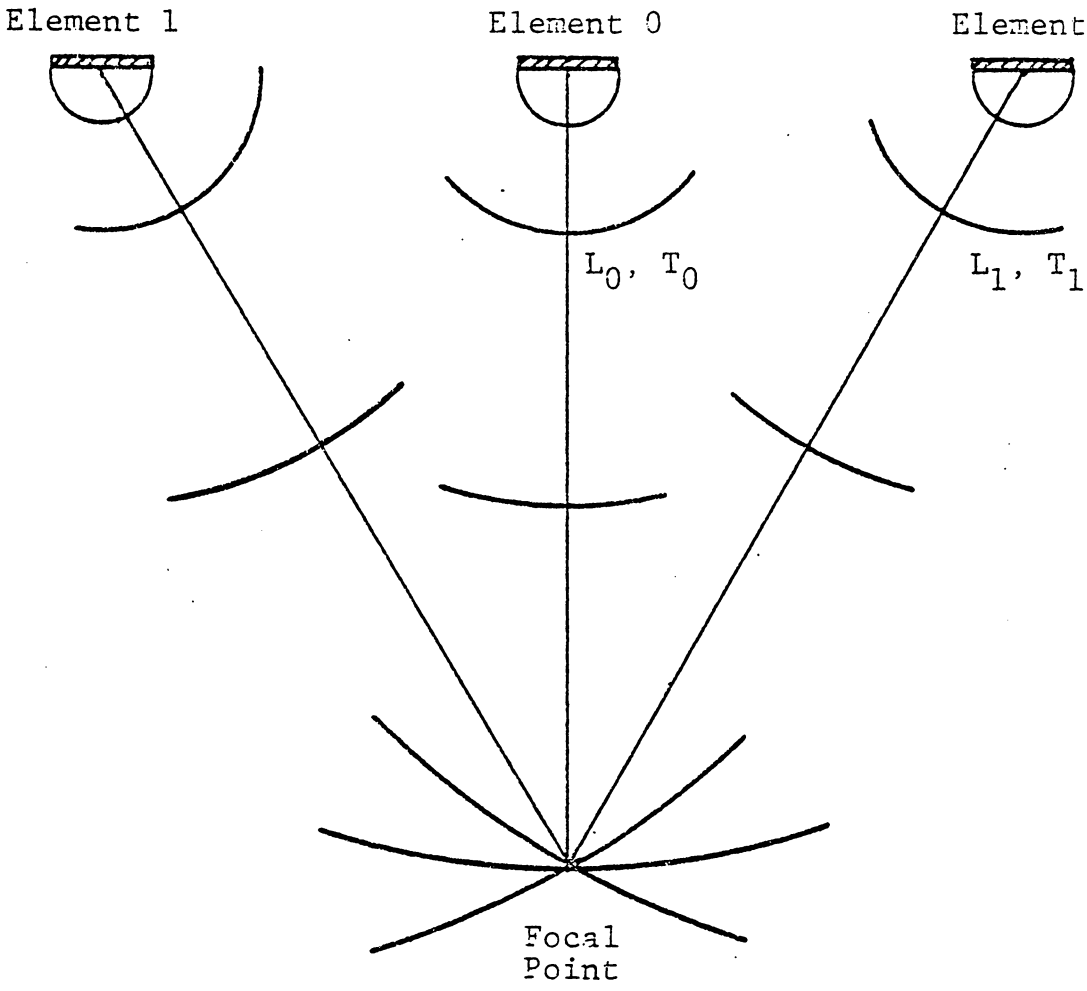

$$\text{Delay} = T_1 - T_0 = \frac{L_1 - L_0}{V_w}$$

Figure 2.13: Axial Focus Geometry

and therefore L_1 needs to be pulsed "delay" seconds before L_0. By carrying out similar calculations, the delay for each ring can be calculated. Because L_0 and the ring radius are known for each ring, the L_n can be calculated using the Pythagorean Theorem. A computer program has been written to calculate delay times before the center spot pulse and has been included in Appendix A.2. Sample timing delays using this program are included in Chapter 5.

Chapter III

RING TRANSDUCER FABRICATION

The ring transducers have different fabrication requirements from conventional uniform transducers. There are two basic types of ring transducer that I have constructed during the past year. The first type is the simple Gaussian profile transducer that does not need to be phased. With these transducers, only a single cable is brought out of the transducer housing. Focusing transducers, on the other hand, need to have a separate coaxial cable for each electrode. Other than the cabling difference, most of the transducer design and fabrication is identical.

The original single-cable Gaussian transducers were half inch diameter crystals and were mounted in a filler loaded epoxy poured into a small piece of PVC plastic pipe. The resistor network was included inside the epoxy [8]. This technique worked but had no provisions for crystal reuse should the design be changed or internal failures occur. The original multi-cable focusing transducer used epoxy and silicon RTV as a backing and sealing material. Unfortunately this did not adhere to the crystal over long periods of time or allow for crystal reuse either. These and other problems have been apparently solved by techniques described below.

3.1 RING DESIGN

The initial step, after specifying transducer resonant frequency and diameter, is to design the ring pattern. If designing a Gaussian transducer, the model RATOM described in Section 2.2 should be used for this purpose. The user iteratively tries various ring radii and widths until satisfied with the fit to a Gaussian function. If a non focusing Gaussian transducer is desired, there should be as few rings as possible and each one should be as wide as possible. This takes later fabrication considerations into account and also provides for maximum acoustical output. Once the number of rings, ring radii, and ring widths are known, an artwork pattern is drawn. This artwork is usually a 5:1 scale India Ink on tracing paper design. This design is then photographically reduced and a proper scale negative made. An example of the artwork is shown in Figure 3.1, but not to scale.

3.2 RING ETCHING

The electrode rings are formed on the piezoelectric transducer element in much the same way as printed circuit board traces are made. To begin with, a uniform coating of metal is deposited on both faces of the element. One face is then coated with a photosensitive etch resistant chemical. This face is here after referred to as the rear face, and will contain the ring electrodes. The photographic negative of the ring pattern is then laid against the rear face and it is exposed to light. After a series of chemical treatments [13], the transducer is etched and the ring electrode pattern remains.

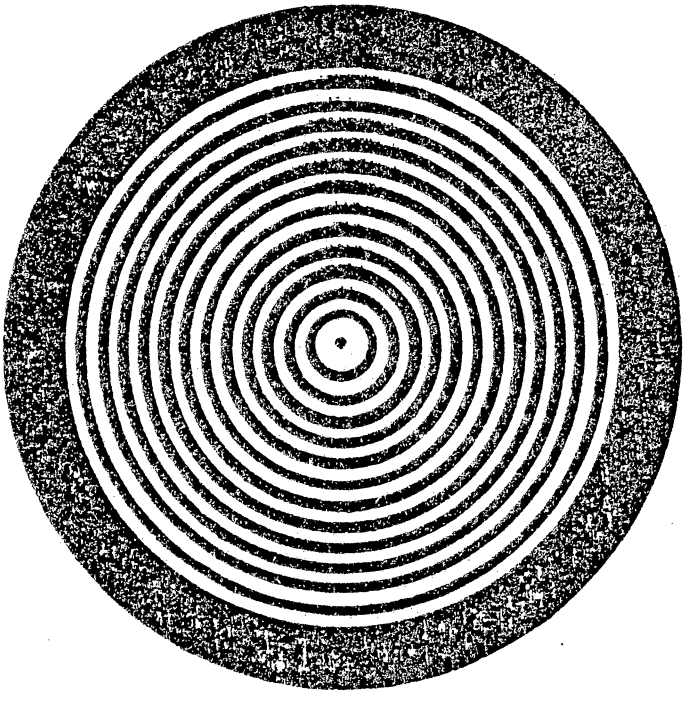

Figure 3.1: Transducer Ring Artwork Pattern

3.3 HOUSING

The transducer housing consists of three major plastic pieces. These can be seen in the cutaway drawing of the completed transducer in Figure 3.2. The major portion of the housing is a section of PVC pipe with an inside diameter slightly larger than the crystal diameter. PVC is used because it is durable, resists cracking, and can withstand immersion in a variety of substances. It is also easy to locate various sizes and is easy to cut and drill. The piezoelectric crystal is mated to the PVC with a plexiglass mounting ring constructed to reasonably tight tolerances. This provides a solid mount that can be accurately sized and aids in establishing a watertight seal around the rear face of the transducer. The mounting ring, lathe cut from half or three-quarter inch plexiglass stock, mates the transducer crystal to the PVC pipe to provide a water tight fit and protect the crystal. The last piece is a thin piece of plexiglass cut to fit the back of the pipe. An ordered sequence of holes, one for each cable in a multi-cable transducer is drilled into this plate. With proper lead attachment, this provides an external display of the cable/electrode relationship, while providing waterproof seals at the back of the transducer and cable strain relief.

3.4 LEAD ATTACHMENT

Lead attachment is a somewhat complicated task due to the multi-electrode configuration. A small framework holds "whisker" wires while they are glued using a conducting epoxy to the transducer electrodes. Soldering or other heat dependent techniques are not practical in most cases. Piezoelectric crystals have thermal expansion coefficients such that uneven heating or cooling will cause a delicate and expensive crystal to crack. We have found that a silver based epoxy, EPO-TEK H20E, is suitable for our purposes. The EPO-TEK epoxy was originally intended for microelectronics substrate bonding. An experimental sample from the microelectronics laboratory proved to have several useful characteristics. This epoxy has a four day curing time which allows a single batch to be mixed when connecting transducer wires. Because this is a delicate and slow procedure, a fast hardening epoxy would be impractical. The EPO-TEK epoxy also has good bond strength to hold the wires once it is hard, yet it does not get brittle. A brittle epoxy (non-conducting) used as a transducer backing and for lead strength on one of the previous experimental transducers delaminated from the transducer crystal, and cracked in many places due to the constant mechanical motion of the piezoelectric crystal.

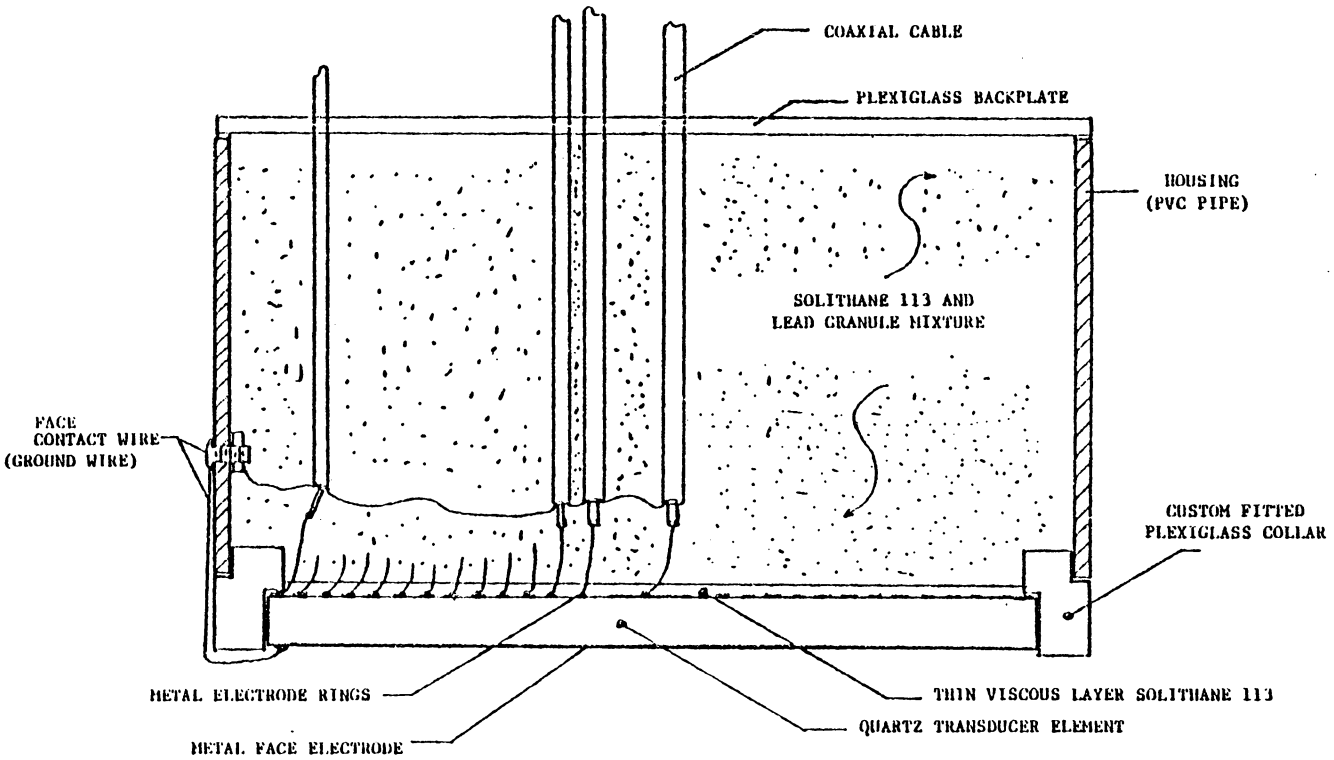

Figure 3.2: Transducer Fabrication Cross Section

3.5 POTTING THE TRANSDUCER ELEMENT

An ideal material to back the transducer element would provide a watertight seal, hold the element in the housing, be nonconducting, and be very dense to increase forward radiated ultrasound. It would also be advantageous if this potting material could be removed at a later time should refabrication become necessary. Consultation with a materials specialist [9] led to the recommendation of Solithane 113, a three part polyurethane mixture. This substance has properties of hardness and curing time that can be controlled by the mixture ratio. Polyurethane is waterproof and provides a good adhesive bond. It does not conduct and can be removed by soaking in acetone. The only desirable feature described above that it does not have is high mass, and therefore would not provide good acoustic backplane loading. We have solved this by mixing lead (Pb) pieces with part of the polyurethane.

The potting process itself is a two stage process. The first stage involves mounting the piezoelectric element with attached leads in the plexiglass mating ring. A thin layer of the polyurethane is poured over the back which glues the element to the plexiglass. This layer provides a watertight seal at the transducer front and an insulating layer over the rings on the back. It also provides additional mechanical stability when working with the whisker wires. The mixture is left slightly viscous to allow it to maintain adhesion during mechanical vibration.

Now that the mounting ring, transducer element and whisker wires form a one-piece unit, any external cables or internal resistor divider networks may be connected. The internal resistor dividers are used to provide Gaussian voltage weighting and are mounted inside the transducer housing. When all internal connections have been made, the mounting ring is affixed to the PVC pipe and the entire pipe section is filled with the polyurethane/lead mixture. A plexiglass back plate is affixed and all possible leaks sealed with externally applied polyurethane.

3.6 INITIAL TESTING

When the polyurethane has hardened, the transducer is ready for its initial testing. This involves testing each ring separately on the multi-cable transducer and a single test for the whole transducer if it is a single cable transducer. Each cable is pulsed, one at a time, and the acoustic output checked with another transducer on the face of the new transducer. This test is merely to make sure that acoustic output exists and all leads appear to be making contact. Initial testing of the prototype 7.62 cm diameter 500 kHz thirteen ring transducer (shown in Figure 3.1) indicated that all rings except ring 2 were operational. Reevaluation using this information in the field prediction algorithm and the focusing algorithm indicated that the transducer could adequately function without ring 2 so refabrication was not necessary. If it passes this test, it is ready for characterization using the automated data system of Chapter IV.

Chapter IV

AUTOMATED TRANSDUCER CHARACTERIZATION

The third major area of research involved developing a means to characterize these various transducers. Complete profile characterization would require knowledge of the acoustic amplitude and phase at every point in a three dimensional solid containing all of the acoustic energy. This amount of information is impractical, however, and need not be acquired. The system which is explained below takes a series of spaced amplitude samples along various lines or planes intersecting this solid. By assuming radial symmetry and continuity between samples, most of the amplitude profile of the transducer can be determined. The system we use does not measure phase information.

4.1 SYSTEM HARDWARE

The characterization system may be broken down into two major components; the source electronics which power the transducer under test, and the detection and processing equipment. The second, the detection and processing equipment, is the more complex of the two. It is composed of many separate subsystems tied together by various data and control signal paths, both analog and digital. It can even control the source electronics under the proper circumstances.

4.1.1 Source Electronics

Depending upon the type of transducer being characterized, this subsystem can vary greatly. For the simplest case of a single-cable transducer, nothing more is needed than a simple pulser or possibly a gated cw signal generator and a power amplifier. For a more complex transducer with individual electrode cables, additional electronics are required. For the uniform focused case operated in pulsed mode, a box has been built utilizing TTL logic timing circuits to create adjustable time delay pulses into high voltage circuits [13]. If it is desired to operate in cw mode, a series of variable-tap high voltage delay lines are needed [2]. It is a relatively simple matter to add additional impedances to each line to adjust the voltage from the pulsing or cw output to the proper levels for a Gaussian beam.

4.1.2 Detectors

The detectors are the first in a large number of subsystems required for signal detection and processing. There have been two distinct methods used in the past year to measure acoustic transducer amplitude at various points in the transmitted field. The first type used another piezoelectric transducer as a receiver, while the second used a laser differential interferometer for the amplitude measurements.

4.1.2.1 Piezoelectric Detector

There were two piezoelectric detectors used. The primary detector was a Harisonics G 0204 2.25 MHz transducer with a small diameter of about 8 mm. This transducer was usually masked with a 3 mm cone which allows a much smaller sample area to be used when the signal strengths are strong enough. In cases where resolution was unimportant but sensitivity was, a 1.4 cm Harisonics V306 2.25 MHz transducer was used. Although these transducers are 2.25 MHz and the source transducers were either 0.500 MHz or 1.00 MHz, this difference does not matter very much for pulsed operation. After receiving the initial pulse, the receiving transducer begins to resonate mechanically and beat a 2.25 MHz signal with the incoming 0.5 MHz signal. Because this effect is the same for every pulse, the relative measurements remain constant with each other.

4.1.2.2 Optical Detection of Acoustic Amplitude

The other major form of detector is an optical system which uses a differential laser interferometer to measure portions of the propagating acoustic energy [4]. The electrical output of the optical system is free of the initial rf pulse which is sensed by the ultrasonic detector, however it typically has a much lower signal-to-noise ratio. This system has the major advantage that it does not interfere with the signal it is measuring because the laser beams do not affect the propagating ultrasonic wave.

4.1.2.3 Water Tank Testing Environments

These transducers have been designed to operate in a liquid environment such as water. The automated testing systems use two water tanks, one a two foot cube of plexiglass with a two-motor two-axis carriage on top. The second is a five feet by one foot by one foot plexiglass and glass tank for far-field measurements using the optical detection system. The optical path scans the ultrasonic beam by use of a single stepper motor.

4.1.3 Analog Signal Processing

The output of both detectors when operating in pulsed mode is a decaying pulse indicative of acoustic amplitude. A sample pulse is shown in Figure 4.1 for the ultrasonic detector system and Figure 4.2 for the optical detector system. These graphs were obtained using the cursor triggering of the Nicolet 2090 digital oscilloscope and the plotter output. A vertical line has been drawn through each graph to indicate where the triggering pulse occurred. The ultrasonically detected pulse, Figure 4.1, consists of an initial burst of rf electromagnetic energy (a), coupled by the water medium. The next portion of the graph, (b), is indicative of the delay due to acoustic propagation and is a function of the distance between the source and receiving transducers. The third portion of the graph is the detected acoustic energy, (c). This contains the information used in later data processing. Our system measures the amplitude of the largest positive peak (d) and

uses this as a relative amplitude measurement. Note the 2.25 MHz beat frequency in each peak following the initial pulse. After the initial acoustic peak, various reflections from the transducers and water boundaries may occur. One reflection is shown in (e). These reflections should be ignored by the data acquisition system.

The optical information, Figure 4.2, is similar, but has a much greater noise level compared to the acoustic peaks. These peaks occur in pairs as the ultrasonic pulse passes through the spatially separated arms of the laser interferometer. The second peak is larger due to constructive interference of the in-phase components continuing to stimulate the first laser probe. The optical system also does not have as large a magnitude electromagnetic pulse and is not as sensitive to reflections.

4.1.3.1 Amplification and Filtering

Both detectors have a very small voltage signal output. The first step in the analog signal processing is to amplify this low-level signal. Multi-stage amplification has proven necessary in order to obtain a signal which can be easily utilized. Immediately following the detector an HP 461A amplifier is used to boost the signal 20 or 40 dB, as necessary. This signal is fed into the main signal processing circuitry, block diagrammed in Figure 4.3. This circuitry is based around a high speed commercial operational amplifier, the LM 318. The first block in the figure is a two-stage cascaded amplifier stage. These amplifiers

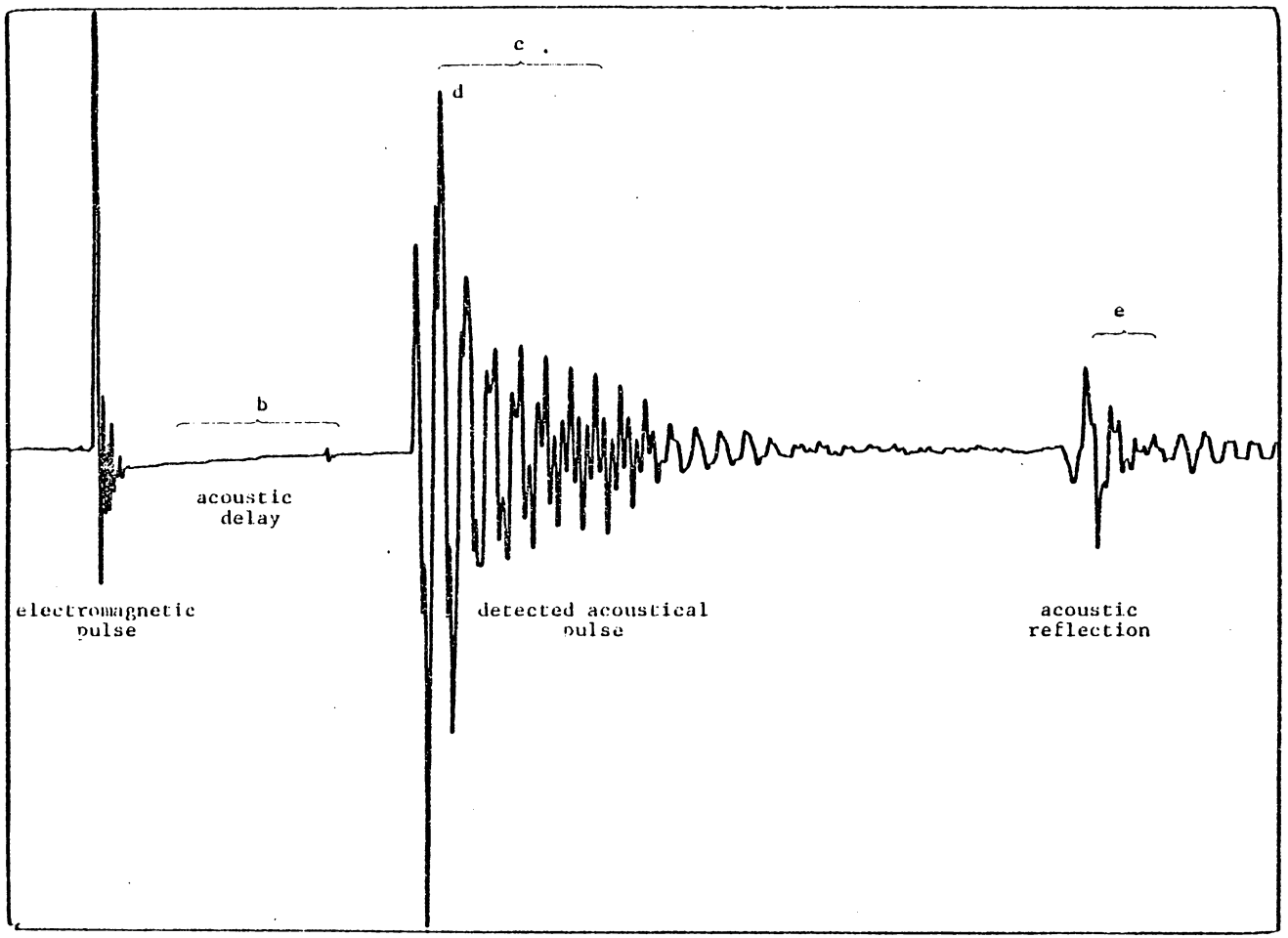

Figure 4.1: Ultrasonically Detected Transducer Pulse

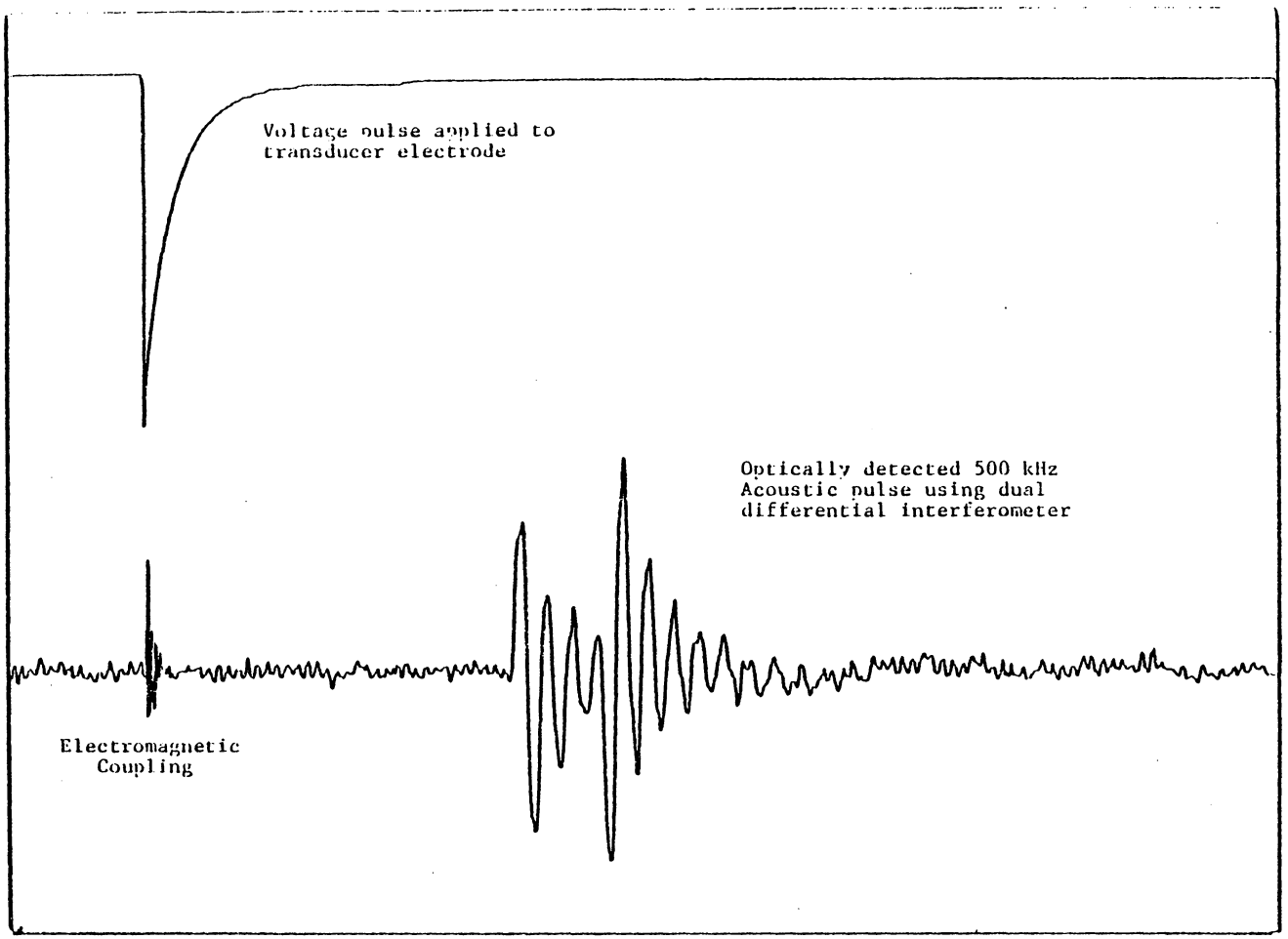

Figure 4.2: Optically Detected Transducer Pulse

each have a voltage gain of between 4 and 5 for a combined voltage gain of about 20. If less signal level is needed at the following stage, the gain can be reduced by a variable potentiometer on the output. Because the LM 318 has a gain-bandwidth product of about 15, this amplifier stage is only good at frequencies below 3 MHz. Most of our pulses are below this frequency range so this is not a problem. In fact, this property actually allows filtering of higher frequency noise that is unnecessary for system operation. Thus, we consider the first stage to be a dual amplifier and low pass filter with cutoff frequency between three and four megahertz.

The third operational amplifier circuit is configured for high pass operation above 10 kHz. Low frequency noise, sometimes referred to as dc noise, is especially prevalent in the optical detection scheme. Vibration caused by movement in the room and near the building can introduce artifact noise into the signal if no filtering protection is provided. A simple high pass filter can remove this noise while continuing to pass the signal information. The combination of a low pass filter cascading a into high pass filter effectively forms a wide band pass filter around the information containing frequencies while rejecting unwanted noise. A gain-frequency plot measured from the final configuration is shown in Figure 4.4. The high pass filter has a bypass switch so that it may be eliminated if unneeded in future experiments that may measure lower frequency information.

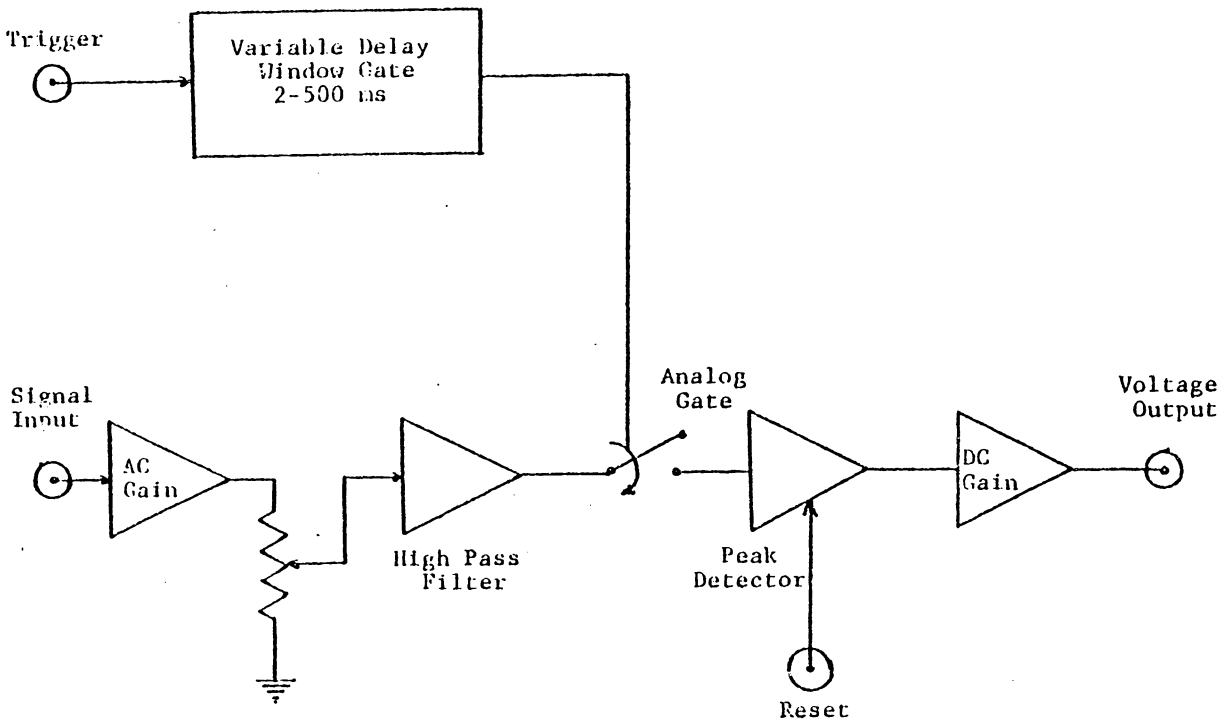

Figure 4.3: Analog Processing Block Diagram

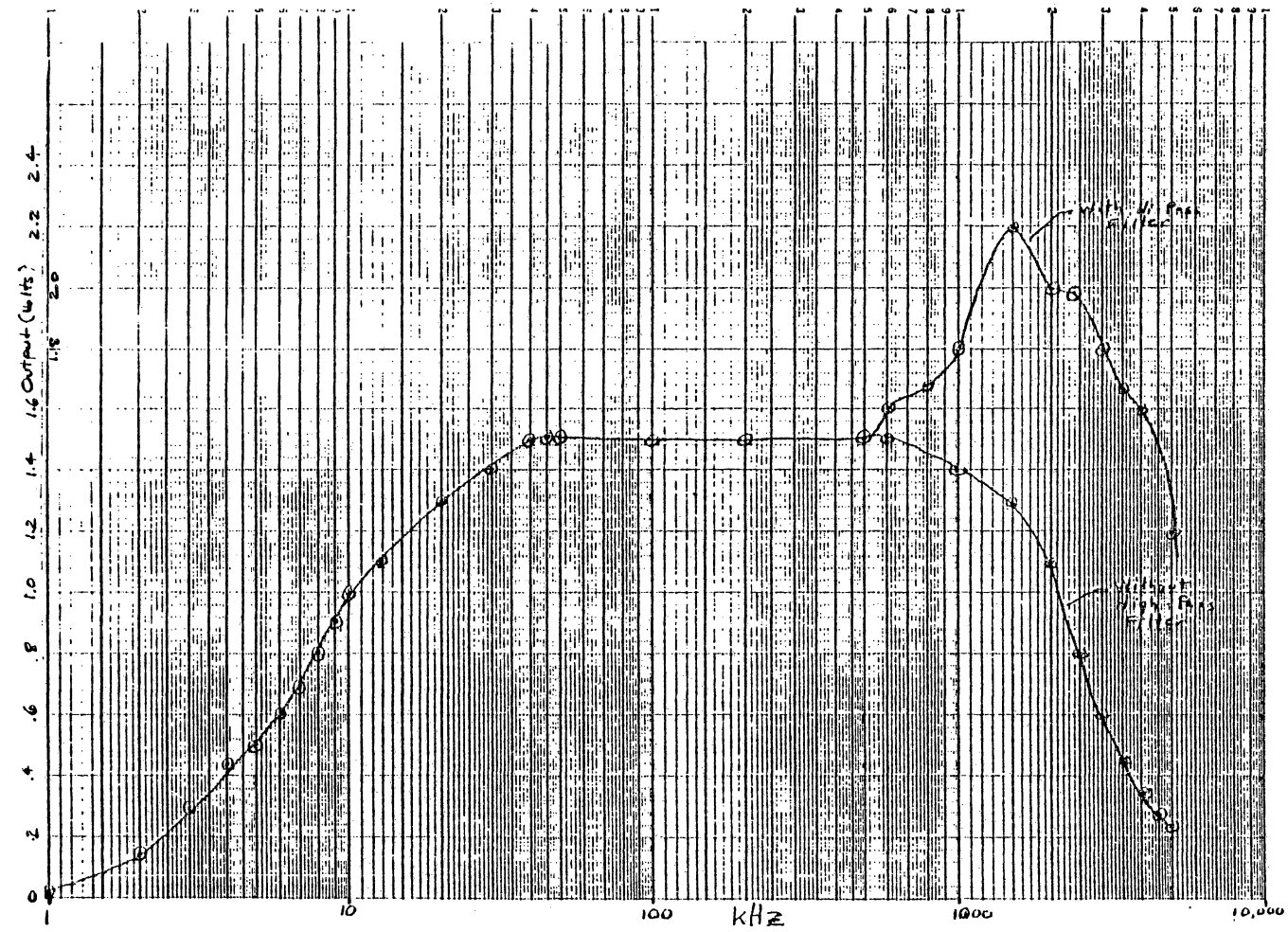

Figure 4.4: Amplifier/Filter Gain-Bandwidth Plot

4.1.3.2 Temporal Filtering

While the frequency domain filters eliminate unwanted frequencies, temporal filtering is needed to eliminate the electromagnetic pulse and any reflections which may be present. Since these signals are all separate on the time axis, this is easily done. The goal is to generate a series of signals which combine to form a single signal that delineates the beginning and ending in time of the desired acoustic pulse. Such a signal may be used to eliminate the remainder of the detected signal which is useless. The procedure is to trigger adjustable one-shots that can mark the beginning and ending of a time window. By logically combining the one-shot signals the window signal can be generated. Two ranges of adjustable one-shot are available, 1-30 ms and 20-500 ms. Since a synchronization pulse is available from the various transducer pulsing circuits, this is the beginning point. The rising edge of this pulse is used to trigger a 74LS123 TTL one-shot, which effectively shortens a variable length synchronization pulse to a 1 ms duration trigger pulse for use by the remainder of the circuitry. Because the acoustic delay can occur anywhere in a 2 to 500 ms range, a combination of the two ranges of the one-shots is needed. The window needs to be "opened" in the full 2 to 500 ms range but can be "closed" in a 20 to 500 ms range without loosing any necessary range. Thus only one circuit is needed to close the window but either the 1-30 ms or the 20-500 ms range may be required to open the window at any one time. A switch was used to select between the two input ranges at any one

time. The 1-30 ms range was achieved with a 74LS123 one-shot while the 20-500 ms range required an NE 555 circuit configured for one-shot operation. By using an NE 556, a dual 555, both the long delay open and the close signal can originate on one chip. Since the 74LS123 is a dual one-shot, one-half is used for signal conditioning and one-half is used for short window open. These chips are wired according to the standard one-shot configuration given in the data books and does not need to be repeated here. The combinational logic is diagrammed in Figure 4.5, along with the FET analog switch used on the detected and filtered ultrasonic signal. A graph of the input signal, window circuit output, and corresponding gated signal is shown in Figure 4.6.

4.1.3.3 The Peak Detector

This amplified, filtered, gated analog signal is now ready for the peak detector circuitry, Figure 4.7. The peak detector output voltage rises with the first positive peak and holds that voltage. If a higher magnitude peak occurs later, the peak detector will ramp up to the higher voltage and hold that. The circuit operation is simple. The output of a unity-gain configuration feeds a capacitor through a fast, low leakage diode. This capacitor charges as the voltage rises but has no low impedance discharge path when the voltage drops. The capacitor voltage is available through a high input impedance op-amp to prevent output loading from degrading circuit performance. Due to various leakage currents, however, the capacitor will slowly discharge.

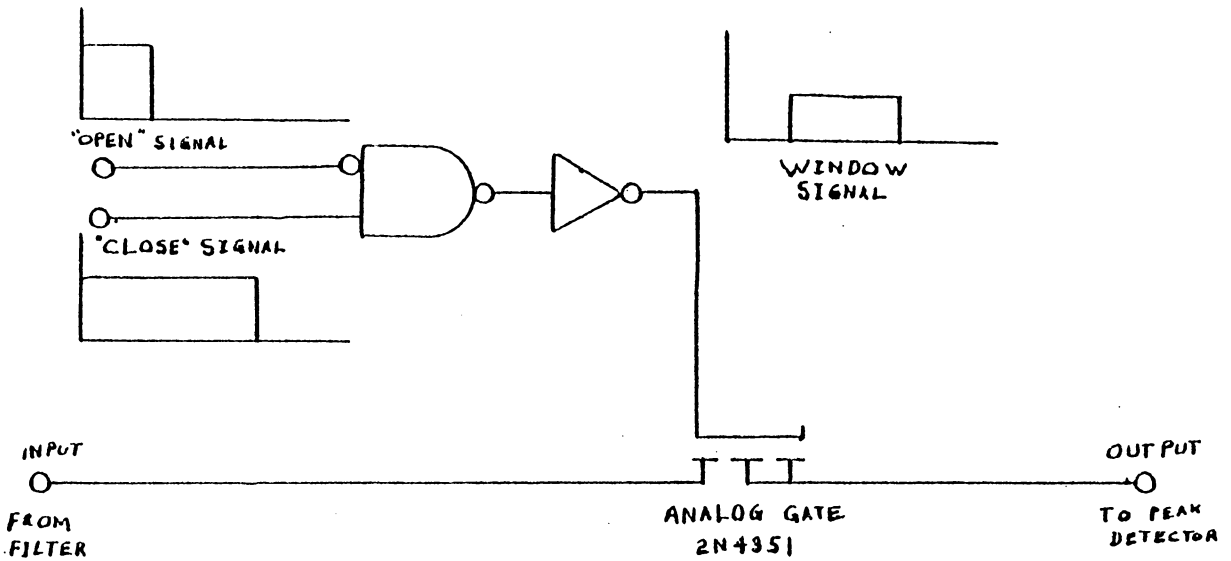

Figure 4.5: Combinational Logic / FET Analog Switch Schematic

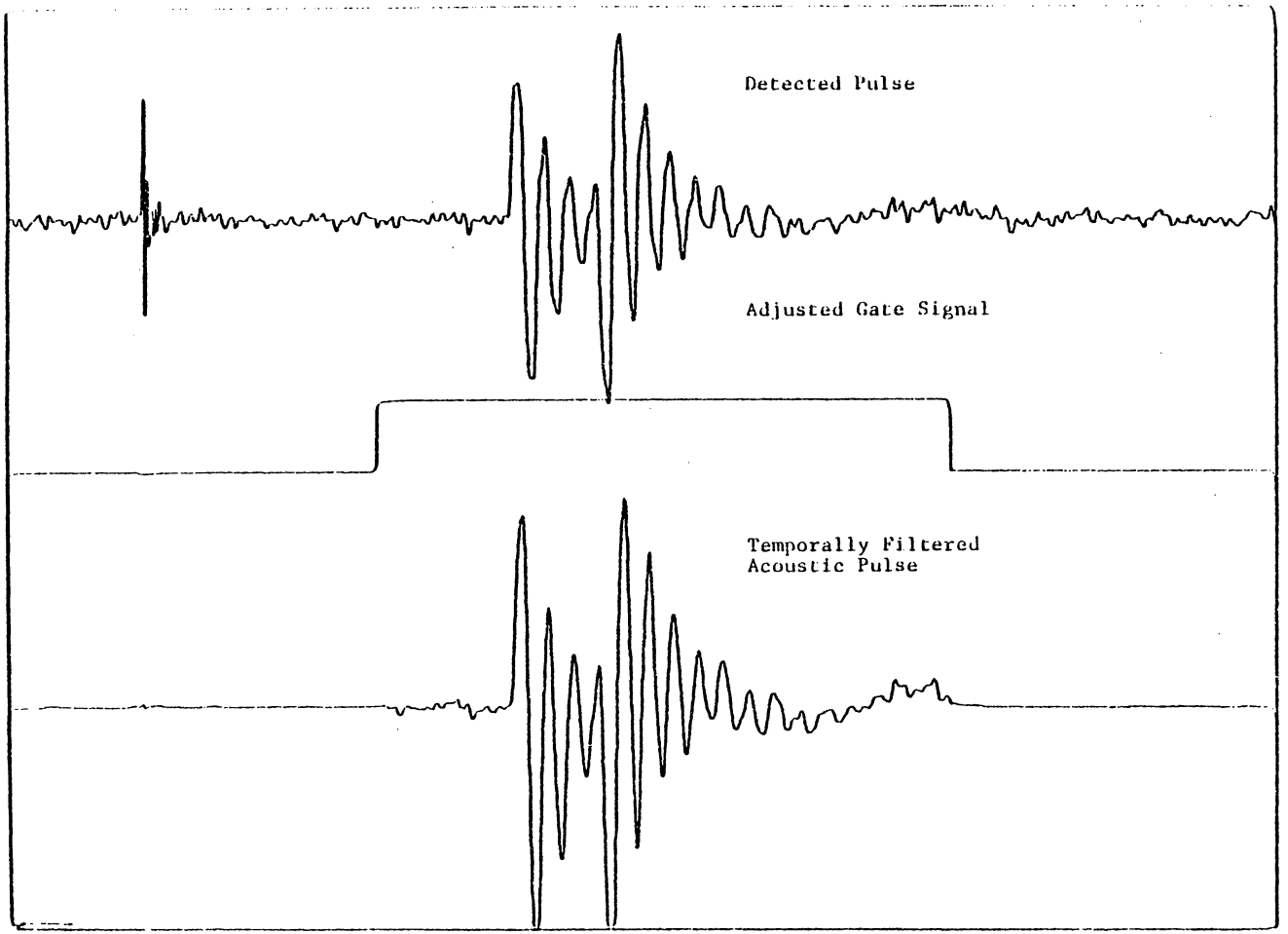

Figure 4.6: Temporally Filtered Acoustic Pulse

The length of time the voltage remains within 90% of the peak voltage is known as the hold time. Longer hold times may be achieved with larger capacitors at the sacrifice of the response time to an input. If longer hold times are necessary, a second stage peak detector can be used. Once the voltage has been measured by an external device, the capacitors are completely discharged through reset transistors and the system is ready for the next peak. In this system the output voltage of the peak detector is fed into an adjustable gain dc amplifier for maximum resolution in the analog-to-digital converter input range.

4.1.4 A/D Conversion

The output of the analog signal processing circuitry is fed into a commercially available analog-to-digital converter, the Cromemco D+7A, with a 0 to 10 volt input range. This A/D board is hardware compatible with the available computer system described in the next section and provides a convenient method of obtaining a digital number corresponding to the peak of the detected acoustic wave.

4.1.5 Microprocessor System

The microprocessor is the central component in the automated transducer characterization system. It performs four primary tasks.

1. It operates as a system manager, linking various subsystems together.

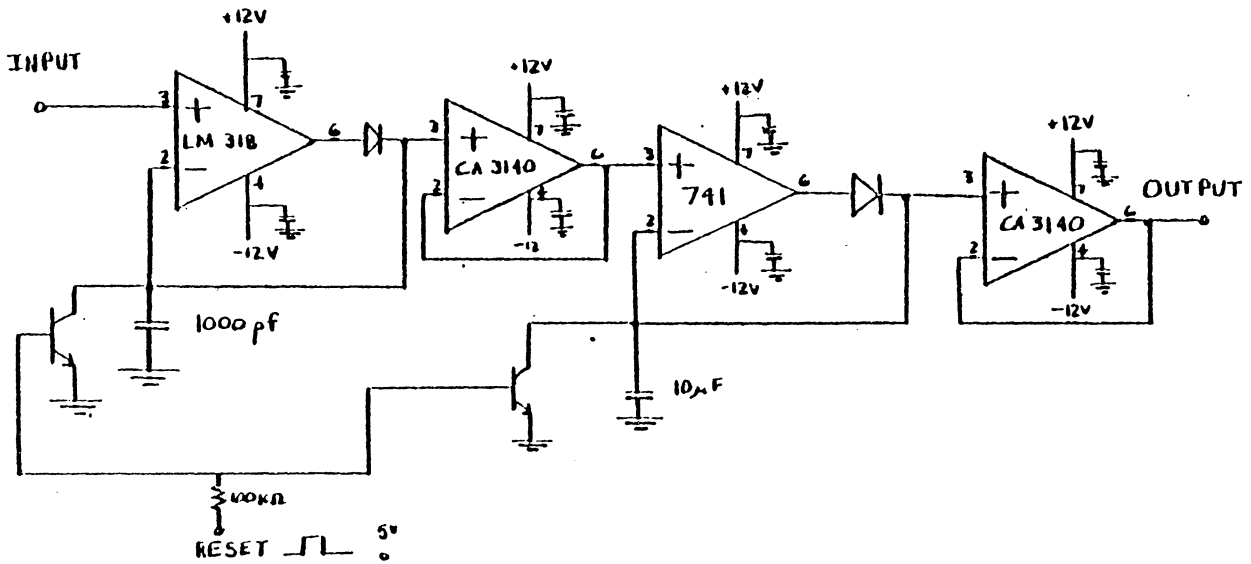

Figure 4.7: Two Stage Peak Detector

2. It controls the motion of the stepper motors and hence the characterization.
3. It provides for data acquisition and storage, and
4. It transfers the stored data for various data processing schemes.

The microprocessor system used is diagrammed in Figure 4.8. The commercial portion consists of a California Computer Systems CCS 2200 mainframe, S-100 motherboard, and power supply. A CCS 2810 4 MHz Z80 Processor card, 65,535 bytes of dynamic RAM and a CCS 2422 floppy disk controller form the heart of the system. A CCS 2710 4-port parallel I/O card and a CCS 2720 four-port serial I/O card provide means of control and communication while the Cromemco D+7A analog-to-digital board is used for data acquisition. The system also has two eight-inch single sided double density 640 KBYTE floppy disk drives and a Zenith Z-29 terminal.

4.1.5.1 System Manager

The system management function does not consist of a specific program or task, but entire system is based around the computer as a controller, data logger, and data manipulator. The fact that the computer can run a variety of languages and be used both to debug hardware as well as operate the final systems gives it a great deal of flexibility.

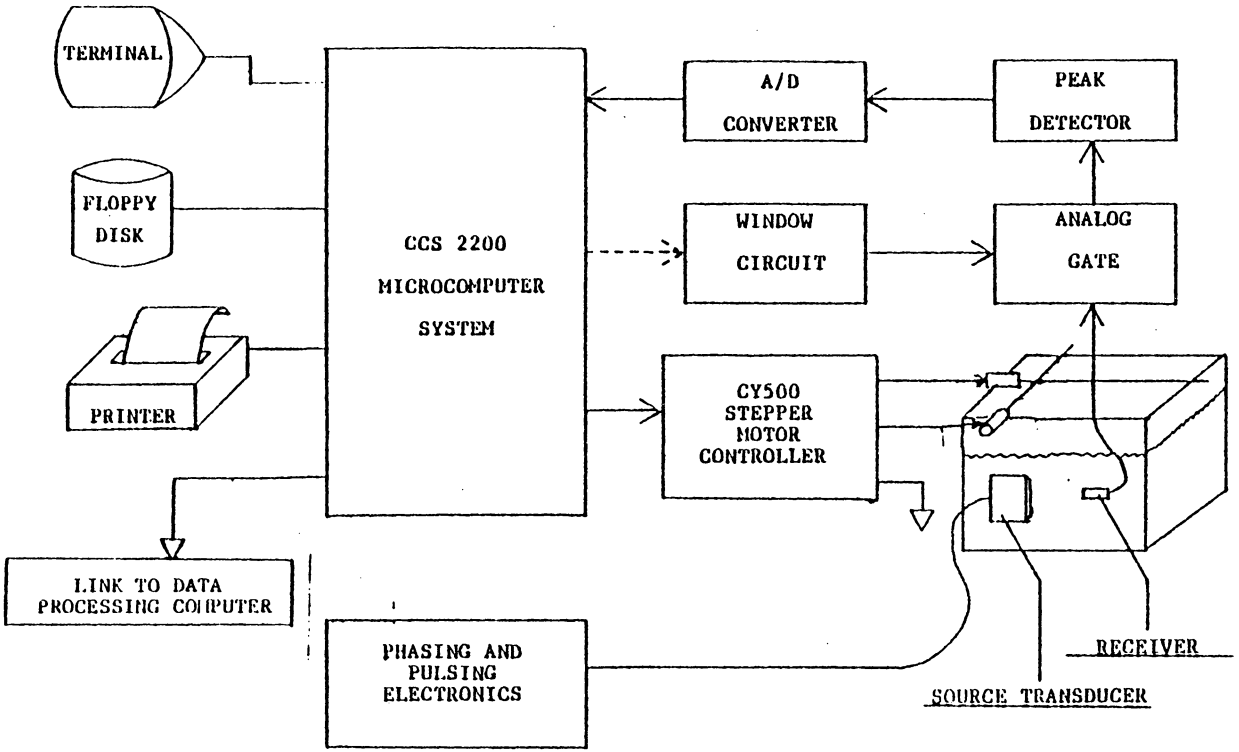

Figure 4.8: Microprocessor Based Data Acquisition System Diagram

4.1.5.2 System Controller

There are several major tasks that are computer controlled. Variable phase delay circuitry may be designed so that the computer can adjust the focal length of a focusing transducer where variable depth is desired. It could also control the various delays used in the window adjustments by calculating the propagation delay time from the source-receiver separation distance. Both of these tasks, however, are currently set manually using an oscilloscope. The two areas of control the computer currently has are in the reset of the peak detector and control of the stepper motor driver circuitry.

The stepper motors are each controlled by a Cybernetic Micro System CY500 Stepper Motor Controller chip. These chips accept higher level ASCII commands over a parallel output data bus and control the step rate and number of steps independent of direct microprocessor monitoring. This frees the microprocessor for other tasks while the stepper motors are moving. The chips each have a small printed circuit board with a data bus, a control bus and a status bus, as well as an output buffer chip and a voltage regulator. An onboard linear select scheme on the control and status busses allows up to four independent motor control axes from one set of I/O ports. Two sets of output pins are provided on each board. One set is directly driven from the four output pins, ϕ_1 - ϕ_4, of the CY500 through a 7405 open collector buffer chip. This can be seen in Figure 4.9, the stepper motor logic schematic. The second set of output pins use only two of the CY500 out-

puts and derive the other two signals necessary through a 7404 inverter. These four signals are then brought to the output pins through the 7405 output buffer as before. The difference is only that when the CY500 outputs are initialized, ϕ_1 - ϕ_4 have the same logic state and the motor is free to move. Using the derived outputs, however, always maintains the motor in a "locked" state when it is not being moved. This is useful under some circumstances such as the optical system's stepper motor configuration. In this system, if the motor is not locked, gravity will cause the optical detector to move and destroy experiment repeatability if not the equipment itself.

The power switching electronics to drive the four phases of the stepper motor is shown in Figure 4.10. Only two phases are shown, because the other two phases use an identical circuit. The dropping resistors are designed to speed up the motor transition between steps and is designed so that it will drop the higher voltage down to the motors specified voltage when in steady state.

4.1.5.3 Data Manipulation

At each position of the stepper motors, a measurement is taken which corresponds to the acoustic wave amplitude at that position. This data is analog processed as discussed in previous sections, and then read into the computer via the analog to digital converter board. The data is then stored on a floppy disk for later transfer to a more sophisticated computer system. This transfer is through one of the serial ports which are attached to the computer system.

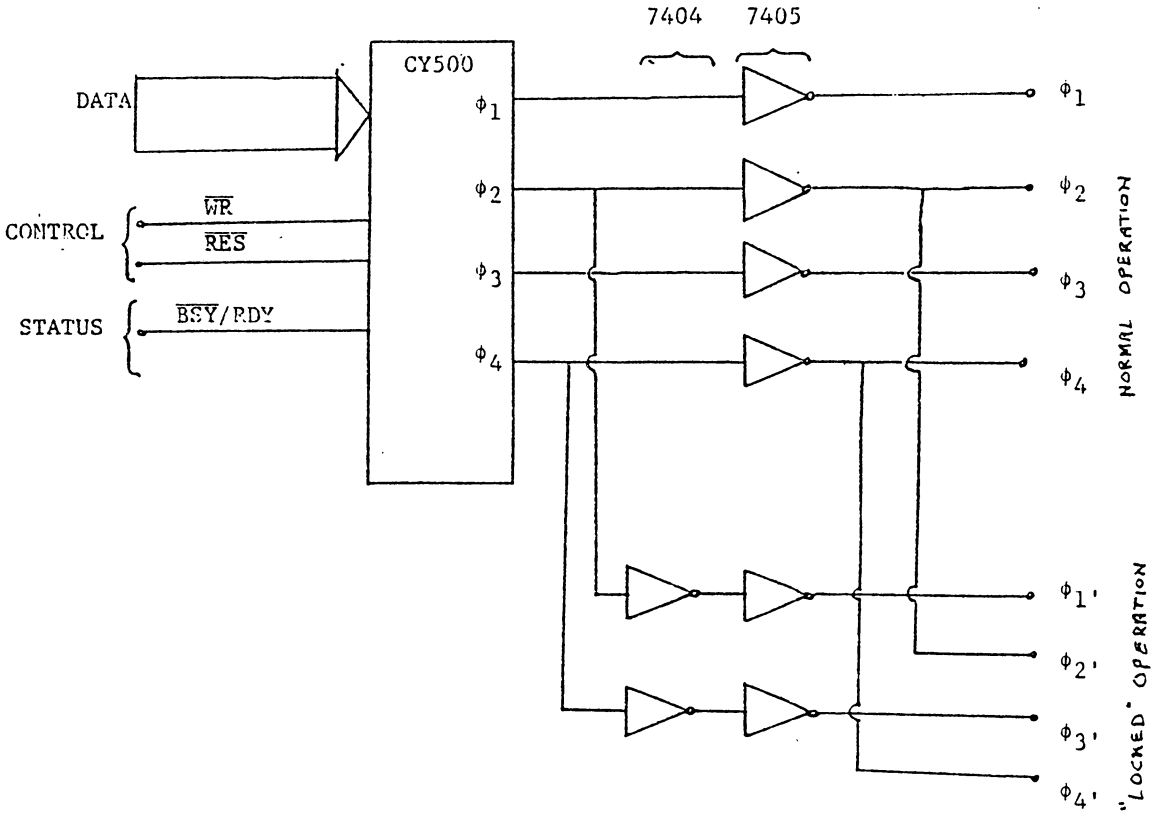

Figure 4.9: Stepper Motor Logic Schematic

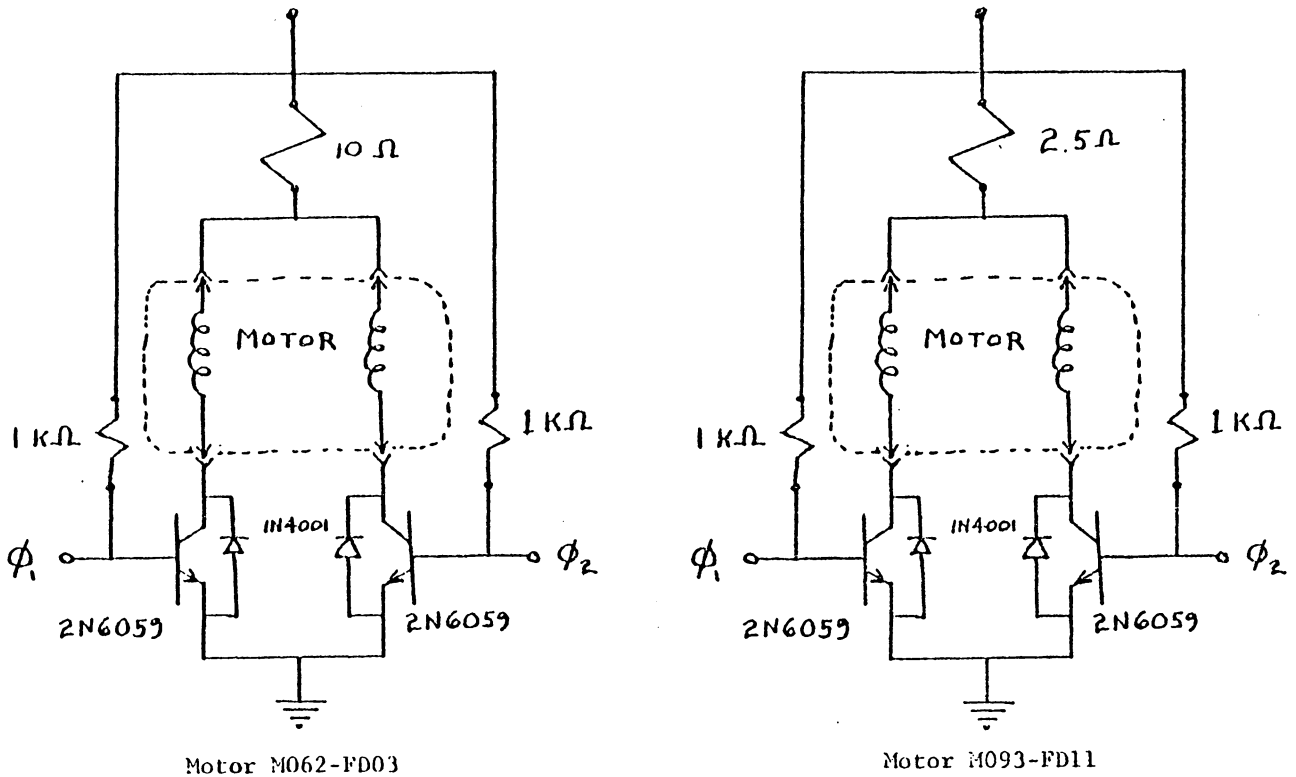

Figure 4.10: Stepper Motor Drive Schematic

4.2 MICROPROCESSOR SOFTWARE

I have spent a great deal of time discussing the hardware of the system. Various design philosophies and system parameters have been explained. This may be useful to later researchers who use the system for transducer characterization. As important as the hardware, however, is the software. The two were each designed with a knowledge of the other to provide an easily used, integrated testing system. The software utilized in this computer consists of both system oriented software such as the BASIC, assembler, and test processing programs as well as application specific programs such as the scanning programs and the various file transfer programs.

4.2.1 Programming Languages

The microprocessor may be programmed as a controller either in assembly language or in BASIC. Unless timing and speed are a factor, BASIC is preferred. BASIC programs are easier to develop and debug, easier to document, and easier to understand previously developed software. BASIC programming also requires only learning how to use BASIC while assembly language programming requires both the text processing program and loading utilities. For these reasons most of the program development has been done using the BASIC language.

4.2.2 Transducer Scanning Software

There are several major programs which are used to control the stepper motors for transducer characterization applications. Examples are given in MAN and SCANX. The first program, MAN, is used for direct manual access to the CY500 command language. This program was primarily used to debug CY500 circuitry and for original motor positioning and movement. A listing of this program is contained in Appendix B.1 for future reference and as an illustration of the principal aspects of a software interface to the CY500 controller chips. The most important segments of the code are the reset routines and the command output routine. Both of these modules are necessary in any program utilizing the CY500's and can be found in all the other programs.

The program SCANX is designed to provide a simple operator interface for manual or automated scans. SCANX, included in Appendix B.2, operates as a controller for a single motor, using the x-axis CY500, to take a one dimensional scan. Such a scan would be the type used by the optical scanning detector which only has one mechanical degree of freedom. An identical program with different constants could control either one of the other axis motors. A simple modification to this program would create SCANXY, expanded to provide for simultaneous two-axis control. This program is divided into two main segments, a motor positioning section and an automated scanning section. The motor positioning section allows relative motor movement specification in millimeters. When the system is positioned to begin the scan, the oper-

ator enters information that completely identifies that scan and then the system performs the automatic scan. The identification information and scan data are stored together in a floppy disk data file for later retrieval. This technique prevents data files from becoming a useless jumble of meaningless numbers to another person at a later date.

4.2.3 Data File Manipulation

After data has been collected and stored on the microprocessor disk system, it must be transferred to another system for processing. It may be needed on either the IBM mainframes for numerical analysis or in the local HP 2647 work station for simple graphical output. Rather than create two transfer programs in the microprocessor and another on the IBM to receive the data, a single program transfers the data to an HP 2647 data tape. The tape may then be read into the IBM using the CMS command 'RDTAPHP <fn> <ft> (MARK'. Although this creates an extra step to transfer data to the IBM, it is simpler and is not as susceptible to IBM operating system changes as a custom data transfer program. The data transfer program, written in BASIC, has the name WRTAPHP to maintain conformity to its CMS command counterpart. Appendix B.3 is the listing.

4.3 DATA PROCESSING

Once the data file has been transferred to the proper machine, it is ready for the appropriate processing. In the case of the HP 2647, the data is plotted as graphical output using the Hewlett-Packard AGL graphics language. A printout of the graph may be obtained for permanent records.

The majority of the data processing, however, is done using the IBM machines. Here the data may be analyzed by curve fitting to the desired function. In the case of two-dimensional scans, the data may be collapsed around to centroid to test the radial symmetry assumption [8]. Data acquired through the optical detector scheme is averaged with several other identical scans to smooth the data and then reconstructed to account for the beam diameter integration inherent with the optical technique [4].

Chapter V

TRANSDUCER SCAN RESULTS

Several transducer scans have been made to validate the theoretical predictions, construction techniques, and scanning equipment. The first transducer scanned using the acoustic detector was the 7.62 cm diameter 13 ring focused uniform case. This transducer was fabricated using the techniques discussed in Chapter 3. Using the timing generation data from the program of Appendix A.2, eight of the ten inner rings were pulsed. The timing used is shown in table 5.1. This was the limit of the available phasing/pulsing equipment. The amplitude graph, Figure 5.1 taken at the focal plane, indicates a good focus. Squaring the amplitude data to yield intensity information resulted in Figure 5.2. From this it was determined that the half power focus diameter was about 3 mm. Thus, a 76.2 mm input was focused to 3 mm, a very good result. Sidelobes, characteristic of uniform amplitude transducers, are visible in both the amplitude and power graphs.

Other scans using this transducer were presented in Section 2.2 to validate the RATOM program. These were taken close to the transducer face to eliminate propagation effects, and are shown in Figure 2.6.

TABLE 5.1

Delay Timings

Ring	Delay, (microseconds)
1	-0.072
2	-0.163
3	-0.285
4	-0.420
5	-0.587
6	-0.741
7	-0.900
8	-1.073
9	-1.237
10	-1.417
11	-1.594
12	-1.769

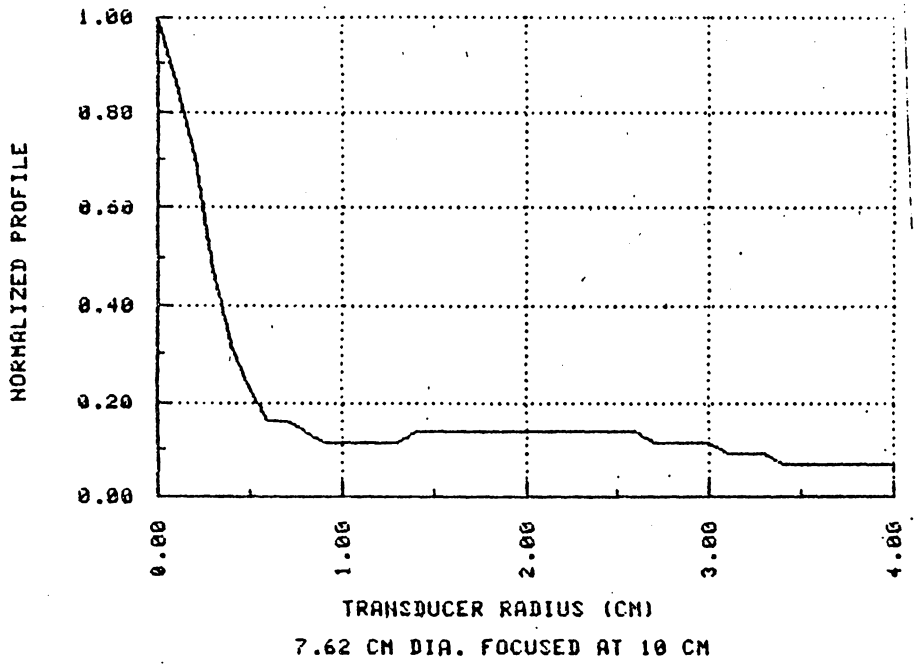

Figure 5.1: Focused Transducer Amplitude Profile

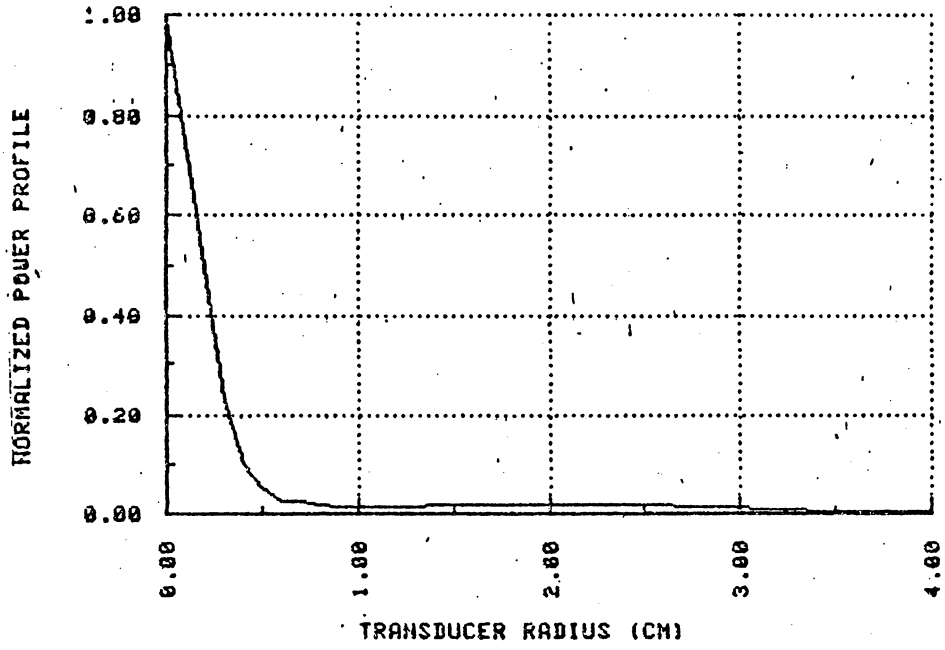

Figure 5.2: Focused Transducer Power Profile

Chapter VI

DISCUSSION OF PROJECT

6.1 CONCLUSIONS

A comprehensive set of design and analysis techniques for variable amplitude and phase transducers have been presented here and in the Master of Science thesis by G. D. Dockery. This work developed a model of the acoustic output of a ring transducer, and means for constructing and testing such transducers. Dockery's work complemented this by developing the propagation theory, the optical detection system, and much of the data analysis algorithms. With the combination of these two it should be possible to completely predict the field of an ultrasonic transducer at any point and validate that prediction experimentally.

The acoustic transducer output model, RATOM, has been very useful in predicting various transducer output characteristics. The fabrication techniques succeeded in producing transducer subsystems which met the goals presented in that section. Finally, the automated data system has progressed well. At the time of this writing, there appear to be several irregularities in some stages of the analog signal processing which prevent unmonitored automatic scanning but these should be worked out soon. The remainder of the system, including the computer system, software, and stepper motor sub-systems, are all working as designed.

6.2 FURTHER RESEARCH AND ADDITIONAL DEVELOPMENT

There are usually as many questions raised by research as are answered and this project has been no exception. The program RATOM has proven a fertile ground for generating potential future applications. These include new developments in Gaussian transducer technology and potential non-Gaussian amplitude distributions. In Gaussian research there are two new approaches to be investigated. The first of these is to impose the condition that each ring and the center spot have equal areas by allowing individual ring widths to vary. This can be done by slight modification to the RATOM program in Appendix A.1. This would mean that each electrode should have equal impedance and ease the design of the voltage divider network. The second Gaussian generation proposal is also to vary the ring widths but maintain uniform voltage on each one. This would eliminate a divider network and simplify construction. A potential non-Gaussian transducer profile that has been mentioned is to utilize many electrodes on a large transducer to generate a

$$\frac{\sin(x)}{x} \tag{6.1}$$

function at the face of the transducer. As this propagates and the Fourier transform occurs, a uniform far field amplitude distribution would occur. This would provide a near-step function far field distribution with no sidelobes and may be almost as advantageous as a Gaus-

sian beam in ultrasonic imaging. If this beam could be focused, even better results could be obtained.

Additional development in some of the instrumentation areas is also possible. A new analog processing circuit, similar to the current one but with several improvements has been proposed by the undergraduate student working in that area. Better results might be obtained by using larger bandwidth circuitry and adjustable bandpass circuitry. There are a multitude of software programs that can be created on the microprocessor and the HP 2647 to control and interface with the current equipment, to operate the Nicolet 2090 digital oscilloscope by remote control, and to communicate between these pieces of equipment with greater flexibility. While there are always improvements that can be made to such a research system, the one developed here has met most of its goals well and should serve its purpose for several years.

Appendix A

TRANSDUCER OUTPUT PREDICTOR PROGRAMS

A.1 RATOM PROGRAM

```
10 REM  ************************************************************
20 REM  *  RATOM: Ring Acoustic Transducer Output Model -           *
30 REM  *   acoustic amplitude profile for concentric ring transducer  *
40 REM  *      BY John W. Gray, III AND William T. O'Connor          *
50 REM  *       COPYRIGHT MARCH 1983                               *
60 REM  *-----------------------------------------------------------*
70 REM  *   VERSION 4.0      FOR H-P 2647A TERMINAL BASIC           *
80 REM  *-----------------------------------------------------------*
90 REM  *   The first few lines are used to define transducer      *
100 REM *    dependant characteristics.  These should be changed   *
110 REM *    by the user for each specific case.                   *
120 REM ************************************************************
130 REM
140 DIM T_out(50),Ideal(50),R_rad(5),R_volt(5),Coeff(5,5),F(5)
150 Radius=6.4  ! Radius of transducer in mm, graph horizontal range
160 Maxvert=1.5 ! Normalized graph maximum value (max y value displayed)
170 Ctrrad=.3  ! Center Spot Radius in mm
180 Nring=4     ! Number of rings, excluding center spot
190 R_wid=.25   ! Ring width in mm
200 Frq=2.25   ! Tranducer natural frequency, in MHz
210 Nstp=25     ! Number of equally spaced intervals on graph
220 Comptr_fit=0 ! 1=Cmptr generate R_volt , 0=User specify R_volt
230 Sfact=.05
240 REM
250 REM
260 R_rad(1)=1.32   !radius of first ring
270 R_rad(2)=2.79   !radius of second ring, etc.
280 R_rad(3)=3.94
290 R_rad(4)=5.16
300 REM
310 REM **** define voltages applied to rings here *****
320 REM           (if user specifying voltages)
330 REM
340 R_volt(0)=1           ! R_volt(1) always 1.0 for normalization
350 IF Comptr_fit=1 THEN 430 ! skip remaining user defines if cmptr fit
360 R_volt(1)=.83
370 R_volt(2)=.46
380 R_volt(3)=.21
390 R_volt(4)=.08
400 REM
410 REM  *** Program defines internal variables here ***
```

```
420 REM
430 Thick=2.86639/Frq  ! Thickness of Crystal
440 R_rad(0)=Ctrrad !center spot radius
450 R_hwid=R_wid/2 ! Half Ring width
460 Maxerr,Err,X,I=0 !these utility variables need to be 0
470 REM
480 REM **** Set up graphics display ****
490 REM
500 PRINT CHR$(232),CHR$(202)  ! Clear Alphanumeric screen
510 PLOTR                        ! reset graphics, clear graphics screen
520 GCLR
530 LOCATE (70,195,20,95)      ! Define Graphics Window
540 SCALE (0,Radius,0,Maxvert) ! Set Scale of Axes
550 FXD (2,2)                  ! Select Axes Labeling Format
560 LAXES (1,.1,0,0,2,2)       ! Define Tic Labels
570 IF Comptr_fit=0 THEN 680    ! skip next section if user defined
580 IF Nring=0 THEN 680        ! voltages or no rings (ctr only)
590 REM
600 REM This section uses Idl_fcn to calculate fit values
610 REM   to pass to solve routine
620 FOR I=0 TO Nring
630 CALL Idl_fcn(R_rad(I),F(I),Sfact,Radius)
640 NEXT I
650 REM
660 CALL Coef(R_rad(),Coeff(,),R_hwid,Thick,Ctrrad,Nring) !Coeff. Matrix
670 CALL Solve(Coeff(,),F(),R_volt(),Nring)  ! solve for voltages
680 REM ***Draw Center spot on  graph ***
690 MOVE (0,1)
700 DRAW (Ctrrad,1)
710 IF Nring=0 THEN 800
720 REM *** Draw individual rings on graph ****
730 FOR I=1 TO Nring
740 X=R_rad(I)
750 R_volt(I)=R_volt(I)/R_volt(0)
760 MOVE (X-R_hwid,R_volt(I))
770 DRAW (X+R_hwid,R_volt(I))
780 NEXT I
790 R_volt(0)=1
800 REM
810 REM **** Plot Ideal Function ****
820 REM
830 I=0
840 MOVE (0,1)
850 LINE (4)              !set dotted line
860 FOR X=0 TO Radius STEP Radius/Nstp
870 CALL Idl_fcn(X,Y,Sfact,Radius)      !calculate value at specified
880 Ideal(I)=Y                          !radius and save in Ideal
890 MOVE (X,Y)                          ! Draw Function
900 PLOT (X,Y)                          ! Draw Function
910 I=I+1                               ! integer index for Ideal
```

```
920 NEXT X
930 REM
940 REM **** Calculate and plot transducer output *********
950 REM
960 REM find output at maximum point (usually X=0) for normalization
970 X=0             !**** set radius of output field maximum here ****
980 CALL Est_output(X,R_rad(),Nring,R_hwid,Thick,R_volt(),Ctrrad,Result)
990 Nrml=1/Result
1000 I=0
1010 MOVE (0,1)
1020 LINE (0)
1030 FOR X=0 TO Radius STEP Radius/Nstp
1040 CALL Est_output(X,R_rad(),Nring,R_hwid,Thick,R_volt(),Ctrrad,Result)
1050 T_out(I)=Result*Nrml       !save output value for error computation
1060 DRAW (X,T_out(I))
1070 I=I+1
1080 NEXT X
1090 REM
1100 REM **** Plot Error ****
1110 REM
1120 I=0
1130 MOVE (0,0)
1140 LINE (6)
1150 Maxerr,Err=0
1160 FOR X=0 TO Radius STEP Radius/Nstp
1170 Err=ABS(Ideal(I)-T_out(I))                              ! Est_output Error
1180 IF Err>Maxerr THEN Maxerr=Err
1190 DRAW (X,Err)
1200 I=I+1
1210 NEXT X
1220 REM
1230 REM **** Label Graph ****
1240 REM
1250 CLIPOFF
1260 LDIR (90)
1270 MOVE (-.15*Radius,.2)
1280 PRINT #0;"NORMALIZED PROFILE";
1290 LDIR (0)
1300 MOVE (.6,-.2)
1310 PRINT #0;"RING RADIUS (mm)";
1320 MOVE (2,1)
1330 PRINT #0;"MAX ERROR = ";Maxerr*100;"%"
1340 PRINT #0;"ACOUSTICAL EFFICIENCY = ";1/(Nrml*3.14159)
1350 PRINT #0;"CRYSTAL  THICKNESS =";Thick;" DIA. =";2*Radius
1360 PRINT #0;"RING WIDTH =";2*R_hwid
1370 MOVE (-.55*Radius,1)
1380 PRINT #0;"RING  RADIUS   VOLTAGE"
1390 IF Nring=0 THEN 1530
1400 PRINT #0;0;SPA(4);Ctrrad;SPA(4);1
1410 FOR I=1 TO Nring
```

```
1420 PRINT #0;I;SPA(4);R_rad(I);SPA(4);R_volt(I)
1430 NEXT I
1440 END
1450 REM ******************************************************  Idl_fcn
1460 REM *                                                        *
1470 REM *       DEFINE FUNCTION YOU WISH TO FIT HERE !!!!!!      *
1480 REM *                                                        *
1490 REM **********************************************************
1500 SUB Idl_fcn(X,Y,Sfact,Radius)
1510 Sigma=-LOG(Sfact)/Radius**2
1520 Y=EXP(-Sigma*X**2)  !Caussian function
1530 REM
1540 SUBEND
1550 SUB Est_output(X,R_rad(),Nring,R_hwid,Thick,R_volt(),Ctrrad,Result)
1560 REM
1570 REM ************************************************** Est_output
1580 REM
1590 Alpha,Beta,Result=0
1600 REM
1610 REM   **** Calculate effect of both sides of ring ***
1620 REM
1630 IF Nring=0 THEN 1700
1640 FOR R=1 TO Nring
1650 CALL R_left(X,Alpha,Beta,R_rad(R),R_hwid,Thick)
1660 Result=Result+(Alpha+Beta)*R_volt(R)
1670 CALL R_right(X,Alpha,Beta,R_rad(R),R_hwid,Thick)
1680 Result=Result+(Alpha+Beta)*R_volt(R)
1690 NEXT R
1700 REM
1710 REM **** Calculate Center Spot as Special Case ****
1720 REM
1730 CALL Ctrspot(X,Ctrrad,Thick,Ctrfld)
1740 Result=Result+(Ctrfld*R_volt(0))
1750 SUBEND
1760 SUB R_left(X,Alpha,Beta,Rad,R_hwid,Thick)
1770 REM
1780 REM ******************************************************  R_left
1790 REM
1800 REM
1810 REM **** Calculate contribution from left half of ring ****
1820 REM
1830 Alpha=ATN((X-(-Rad-R_hwid))/Thick)
1840 Beta=ATN(((-Rad+R_hwid)-X)/Thick)
1850 SUBEND
1860 SUB R_right(X,Alpha,Beta,Rad,R_hwid,Thick)
1870 REM
1880 REM ***************************************************** R_right
1890 REM
1900 REM
1910 REM **** Calculate contribution from right half of ring ****
```

```
1920 REM
1930 Alpha=ATN((X-(Rad-R_hwid))/Thick)
1940 Beta=ATN(((Rad+R_hwid)-X)/Thick)
1950 SUBEND
1960 SUB Ctrspot(X,Rad,Thick,Ctrfld)
1970 REM
1980 REM ************************************************** Ctrspot
1990 REM
2000 REM **** Special Case of Center Spot ****      ! Value returned in
2010 REM                                           ! Ctrfld.
2020 Xp=X
2030 Ctrfld=0
2040 A=.6*Rad                                      !******************
2050 C=Rad                                         ! Divide Center Spot
2060 CALL Rect_fld(A,Thick,C,Xp,E)                 ! into closely approx
2070 Ctrfld=E                                     ! rectangles & call
2080 A=.14*Radc=.64*Rad                           ! Rect_fld for exact
2090 Xp=X-.72*Rad                                 ! output for each rect
2100 CALL Rect_fld(A,Thick,C,Xp,E)                !******************
2110 Ctrfld=Ctrfld+E
2120 Xp=X+.72*Rad
2130 CALL Rect_fld(A,Thick,C,Xp,E)
2140 Ctrfld=Ctrfld+E
2150 Xp=X-.88*Rad
2160 A=.08*Radc=.36*Rad
2170 CALL Rect_fld(A,Thick,C,Xp,E)
2180 Ctrfld=Ctrfld+E
2190 Xp=X+.88*Rad
2200 CALL Rect_fld(A,Thick,C,Xp,E)
2210 Ctrfld=Ctrfld+E
2220 SUBEND
2230 SUB Rect_fld(A,B,C,Xp,E)
2240 REM
2250 REM ************************************************** Rect_fld
2260 REM
2280 B2=B**2
2290 C2=C**2
2300 Aminx=A-Xp
2310 Aplusx=A+Xp
2320 Temp=C*Aminx/((B2+C2)**.5*(Aminx**2+B2)**.5)      ! Arcsine function
2330 Alph=ATN(Temp/(1-Temp**2)**.5)                   !****************
2340 Temp=C*Aplusx/((B2+C2)**.5*(Aplusx**2+B2)**.5)
2350 Bet=ATN(Temp/(1-Temp**2)**.5)
2360 E=Alph+Bet
2370 SUBEND
2380 SUB Coef(R_rad(),Coeff(,),R_hwid,Thick,Ctrrad,N)
2390 REM
2400 REM ************************************************** Coef
2410 REM
2420 REM
```

```
2430 REM **** Calculate the Coefficient Matrix ****     ! Values returned
2440 REM                                                ! in Coeff(,).
2450 FOR I=0 TO N
2460 CALL Ctrspot(R_rad(I),Ctrrad,Thick,Ctrfld)
2470 Coeff(I,0)=Ctrfld
2480 FOR J=1 TO N
2490 CALL R_left(R_rad(I),Alpha,Beta,R_rad(J),R_hwid,Thick)
2500 Coeff(I,J)=Alpha+Beta
2510 CALL R_right(R_rad(I),Alpha,Beta,R_rad(J),R_hwid,Thick)
2520 Coeff(I,J)=Alpha+Beta+Coeff(I,J)
2530 NEXT J
2540 NEXT I
2550 SUBEND
2560 SUB Solve(A(,),B(),X(),Ncol)
2570 REM
2580 REM ************************************************** Solve
2590 REM
2600 REM                                        ! A(,)->Matrix of Coef.
2610 REM **** Solve for Ring Potentials ****    ! B() ->Forcing Function
2620 REM                                        ! X() ->Solution Vector
2630 Er=0                                       ! Ncol->dimension of array
2640 FOR I=0 TO Ncol-1                          ! Er  ->error flag
2650 I1=I+1
2660 FOR J=I1 TO Ncol          ! this routine uses a simple gaussian
2670 T=A(J,I)/A(I,I)           ! elimination routine to solve for
2680 FOR K=I1 TO Ncol          ! the proper ring voltages.
2690 A(J,K)=A(J,K)-T*A(I,K)
2700 NEXT K
2710 B(J)=B(J)-T*B(I)
2720 NEXT J
2730 NEXT I
2740 IF A(Ncol,Ncol)=0 THEN Er=1 ELSE GOSUB 2770
2750 IF Er=1 THEN PRINT ERROR: Singular matrix, no fit possible. STOP
2760 GOTO 2860
2770 X(Ncol)=B(Ncol)/A(Ncol,Ncol)
2780 FOR I=Ncol-1 TO 0 STEP -1
2790 Result=0
2800 FOR J=I+1 TO Ncol
2810 Result=Result+A(I,J)*X(J)
2820 NEXT J
2830 X(I)=(B(I)-Result)/A(I,I)
2840 NEXT I
2850 RETURN
2860 SUBEND
```

A.2 DELAY PROGRAM

```
10 REM ******************************************************
20 REM *  DELAY:  CALCULATE DELAYS FOR PULSED FOCUSING      *
30 REM *          TRANSDUCER BASED ON HILDEBRAND GEOMETRICAL *
40 REM *          APPROXIMATION.                             *
50 REM *                                                     *
60 REM *   BY JOHN GRAY     MAY, 1983                       *
70 REM *                                                     *
80 REM ******************************************************
90 REM
100 REM OUTER RINGS ARE PULSED FIRST WHILE CENTER SPOT IS
110 REM PULSED LAST, HOWEVER DUE TO PULSING PRIORITIES, IT
120 REM IS BETTER TO PULSE INNER RINGS WHEN ALL RINGS CANNOT
130 REM BE PULSED. THIS PROGRAM GENERATES TIMING DELAYS
140 REM BASED ON CENTER SPOT PULSED AT TIME T=0. SINCE ALL
150 REM OTHER RINGS ARE  PULSED BEFORE THIS, THEY HAVE A
160 REM NEGATIVE DELAY TIME.
170 REM
180 NRING=12                  ! NUMBER OF RINGS
190 DIM RAD(15)               ! INDIVIDUAL RING RADII (MM)
200 RAD(0)=3.3147             ! CENTER SPOT RADIUS
210 RAD(1)=4.6736             ! RING 1 RADIUS, ...ETC
220 RAD(2)=7.239
230 RAD(3)=9.906
240 RAD(4)=12.4986
250 RAD(5)=15.4432
260 RAD(6)=18.0086
270 RAD(7)=20.574
280 RAD(8)=23.2918
290 RAD(9)=25.8318
300 RAD(10)=28.575
310 RAD(11)=31.242
320 RAD(12)=33.8582
330 FOCAL=10                   !FOCAL LENGTH DESIRED
340 VELOCITY=1430*100          !VELOCITY OF SOUND IN WATER, 1430 CM/SEC
350 TIMEO=FOCAL/VELOCITY       !PROPAGATION TIME FROM CENTER OF XDCR
                                TO FOCUS
360 PRINT "RING","DELAY (MICROSEC)"       !PRINT HEADINGS
370 FOR I=1 TO NRING                      !SOLVE FOR EACH RING DELAY
380 TIME=(RAD(I)**2+FOCAL**2)**.5/VELOCITY  !PROPAGATION TIME FROM RING "I"
390 DELAY=TIMEO-TIME                      !DELAY FROM CTRSPOT PROP. TIME
400 PRINT I,DELAY*10000                 !PRINT RING, DELAY IN MICROSECONDS
410 NEXT I
```

Appendix B

MICROPROCESSOR CONTROL SOFTWARE

B.1 MAN PROGRAM

```
10 REM
20 REM MAN : MANUAL CONTROL PROGRAM FOR CY500'S. ALLOWS CY500 COMMANDS
30 REM TO BE PASSED DIRECTLY TO CY500 DATA PORT. LINE EDITING MAY
40 REM BE DONE BEFORE THE RETURN KEY IS HIT. SPECIAL FEATURES ARE:
50 REM   BYE : WILL RESET CY500 AND EXIT PGM
55 REM
56 REM  BY JOHN GRAY  FALL 1982
57 REM
60 OUT 238,255
70 OUT 238,1
80 FOR I=1 TO 10
90 NEXT I
100 OUT 238,&H11
110 C$=CHR$(13)
120 FOR I=1 TO 100
130 NEXT I
140 REM INITIALIZATION STRING
150 INIT$="I"+C$+"F 1"+C$+"R 238"+C$+"N 200"+C$
160 FOR I=1 TO LEN(INIT$)
170 CHAR=ASC(MID$(INIT$,I,1))
180 GOSUB 300
190 NEXT I
200 INPUT A$
210 IF A$="BYE" THEN 360
220 FOR I=1 TO LEN(A$)
230 CHAR=ASC(MID$(A$,I,1))
240 GOSUB 300
250 NEXT I
260 CHAR=13
270 GOSUB 300
280 GOTO 200
290 REM OUTPUT CHARACTER TO CY500
300 OUT 239,CHAR : OUT 238,&H10
310 IF (INP(238) AND 1)=1 THEN 310
320 OUT 238,&H11
330 IF (INP(238) AND 1)=0 THEN 330
340 RETURN
350 REM RESET LOOP
360 OUT 238,1
370 FOR I=1 TO 10
380 NEXT I
```

```
390 OUT 238,&H11
```

B.2 SCANX PROGRAM

```
10 REM  ************************************************************
20 REM  *                                                          *
30 REM  *   PROGRAM:   SCAN-X                                      *
40 REM  *                                                          *
50 REM  *      MOVES "X" MOTOR MANUALLY TO DO INITIAL POSITIONING, *
60 REM  *      THEN TAKES DATA SCAN AND STORES ON DISK.            *
70 REM  *                                                          *
80 REM  *     BY  JOHN GRAY       FEBRUARY 1983                  *
90 REM  *                                                          *
100 REM ************************************************************
110 REM
120 REM  CY500 INPUT/OUTPUT PORTS. 'X' IS BITS 0 AND 4; 'Y' IS BITS 1,5
130 REM   238 OUTPUT: CONTROL PORT
140 REM       BITS 0-3, WRITE BITS
150 REM       BITS 4-7, RESET BITS
160 REM   238 INPUT:  STATUS PORT
170 REM       BITS 0-3, BUSY/READY
180 REM       BITS 4-7, ABORT SWITCH
190 REM   239 OUTPUT:   DATA OUT
200 REM
210 REM SET UP CONSTANTS FOR USE IN PGM
220 REM
230 C$=CHR$(13)  'DEFINE CARRIAGE RETURN CHARACTER
240 CLR$=CHR$(27)+"H"+CHR$(27)+"J"
250 R$=""
260 PRINT CLR$;"Are you using large or small motors (L or S)";
270 INPUT LS$
280 IF LS$="L" THEN R$="233" : SCALE=29.28
290 IF LS$="S" THEN R$="244" : SCALE=157.5
300 IF R$="" THEN 260
310 REM
320 REM RESET CY500 (LOOP MUST LAST MINIMUM 10 MILLISEC)
330 OUT 238,&HF
340 FOR I=1 TO 15
350 NEXT I
360 OUT 238,&HF1
370 REM
380 FOR I=1 TO 15
390 NEXT I
400 REM SEND INITAILIZATION STRING TO CY500
410 CMD$="I"+C$+"F 1"+C$+"R "+R$+C$+"N 200"
420 GOSUB 2210
430 IF LS$="L" THEN CMD$="-"+C$+"0":GOSUB 2210
440 REM
450 REM   ALLOW USER TO POSITION MOTOR PRIOR TO SCAN
460 REM
470 PRINT CLR$
480 PRINT "Give signed number to indicate direction"
```

```
490 PRINT "and number of millimeters to move. Use 0"
500 PRINT "to indicate when ready for automatic scan."
510 PRINT "A null line will cause the same move to be repeated."
520 PRINT "(Scan may be aborted at any time by typing <cntl>-C)"
530 PRINT
540 INPUT "Move";N$
550 IF N$="+" THEN CMD$="+" : GOSUB 2210 : N$=""
560 IF N$="-" THEN CMD$="-" : GOSUB 2210 : N$=""
570 IF N$="" THEN CMD$="G" : GOSUB 2210 : GOTO 530
580 IF N$="I" THEN CMD$="I" : GOSUB 2210 : GOTO 10
590 IF N$="0" THEN 670
600 N=VAL(N$)
610 IF N>0 THEN CMD$="+" : GOSUB 2210
620 CMD$="N"+STR$(ABS(CINT(N*SCALE)))+C$+"G"
630 GOSUB 2210
640 GOTO 530
650 PRINT "ERROR ON INPUT, MUST BE NUMERIC OR NULL, REDO"
660 GOTO 530
670 INPUT "Are you ready to scan";YN$
680 IF MID$(YN$,1,1)<>"Y" THEN 480
690 PRINT CLR$
700 INPUT "What are your initials";INITL$
710 IF LEN (INITL$)>3 THEN
720 ON ERROR GOTO 1570
730 OPEN "I",#2,"SCN."+INITL$
740 INPUT #2,FIL$,NAM$,DAT$,XDCR$,DIA,FREQ$,DIST,STP,NSTEPS
750 INPUT #2,RCVR$,MSK$,FOCUS$,COMMENT$
760 PRINT CLR$;"Last data file was ";FIL$
770 INPUT "Filename to store scan data (filetype of .DAT assumed)";FIL$
780 FIL$=FIL$+".DAT"
790 ON ERROR GOTO 870
800 OPEN "I",#1,FIL$
810 CLOSE
820 PRINT CLR$
830 PRINT "ERROR, FILE ";FIL$;" ALREADY EXISTS. CHOOSE NEW FILE NAME"
840 INPUT "NEW FILE NAME";FIL$
850 FIL$=FIL$+".DAT"
860 GOTO 800
870 RESUME 880
880 ON ERROR GOTO 0
890 CLOSE
900 IF FIL$="" THEN 770
910 PRINT CLR$;"The file ";FIL$;" will contain the scan data."
920 PRINT "Scan date is ";DAT$
930 PRINT "Source transducer configuration: ";XDCR$;",";DIA;"cm diameter"
940 PRINT "Operating at ";FREQ$
950 PRINT "The scan will be taken at ";DIST;"cm, with ";STP;"mm between data samples"
960 PRINT "A total of ";NSTEPS;" data samples will be taken."
970 PRINT "The detector is the ";RCVR$;
980 IF MSK$<>"" THEN PRINT " masked by ";MSK$;
```

```
990 PRINT "."
1000 IF FOCUS$<>"" THEN PRINT "Focussed at ";FOCUS$;"cm."
1010 PRINT COMMENT$
1020 PRINT
1030 INPUT "Are all these parameters OK";YN$
1040 IF MID$(YN$,1,1) = "Y" THEN 1670
1050 IF MID$(YN$,1,1) <> "N" THEN 910
1060 PRINT CLR$
1070 PRINT "Hit RETURN key to accept the value in parenthesis for"
1080 PRINT"each value listed after the question, otherwise type"
1090 PRINT"the new value to change it."
1100 PRINT "To eliminate unused variables, type an 'X'"
1110 P1$="("
1120 P2$=")"
1130 PRINT
1140 PRINT "Data file ";P1$;FIL$;P2$;
1150 INPUT X$
1160 IF X$<>"" THEN FIL$=X$+".DAT"
1170 PRINT "Your Name ";P1$;NAM$;P2$;
1180 INPUT X$
1190 IF X$<>"" THEN NAM$=X$
1200 PRINT "Today's Date ";P1$;DAT$;P2$;
1210 INPUT X$
1220 IF X$<>"" THEN DAT$=X$
1230 PRINT "Source Transducer ";P1$;XDCR$;P2$;
1240 INPUT X$
1250 IF X$<>"" THEN XDCR$=X$
1260 PRINT "Source Transducer diameter ";P1$;DIA;"cm";P2$;
1270 INPUT X
1280 IF X<>0 THEN DIA=X
1290 PRINT "Source Transducer frequency ";P1$;FREQ$;P2$;
1300 INPUT X$
1310 IF X$<>"" THEN FREQ$=X$
1320 PRINT "Scan Distance ";P1$;DIST;"cm";P2$;
1330 INPUT X
1340 IF X<>0 THEN DIST=X
1350 PRINT "Step Size ";P1$;STP;"mm";P2$;
1360 INPUT X
1370 IF X<>0 THEN STP=X
1380 PRINT "Number of data samples ";P1$;NSTEPS;P2$;
1390 INPUT X
1400 IF X<>0 THEN NSTEPS=X
1410 PRINT "Detector ";P1$;RCVR$;P2$;
1420 INPUT X$
1430 IF X$<>"" THEN RCVR$=X$
1440 PRINT "Masked by ";P1$;MSK$;P2$;
1450 INPUT X$
1460 IF X$<>"" THEN MSK$=X$
1470 IF X$="X" THEN MSK$=""
1480 PRINT "Focal Length ";P1$;FOCUS$;"cm";P2$;
```

```
1490 INPUT X$
1500 IF X$<>"" THEN FOCUS$=X$
1510 IF X$="X" THEN FOCUS$=""
1520 PRINT "Additional comments ";P1$;COMMENT$;P2$;
1530 INPUT X$
1540 IF X$<>"" THEN COMMENT$=X$
1550 IF X$="X" THEN COMMENT$=""
1560 GOTO 790
1570 IF ERR=53 THEN 1590
1580 ON ERROR GOTO 0
1590 PRINT "No prior scan information is available for initials '";INITL$;"'"
1600 PRINT "If these are incorrect, type <cntl>-C and restart program."
1610 PRINT "Otherwise, a file SCN.";INITL$;" will be created from your "
1620 PRINT "responses to the following questions. Any that do not apply,"
1630 PRINT "respond with a carriage return."
1640 P1$=""
1650 P2$=""
1660 RESUME 1170
1670 OPEN "O",#2,"SCN."+INITL$
1680 WRITE#2,FIL$,NAM$,DAT$,XDCR$,DIA,FREQ$,DIST,STP,NSTEPS
1690 WRITE#2,RCVR$,MSK$,FOCUS$,COMMENT$
1700 CLOSE #2
1710 OPEN "O",#1,FIL$
1720 WRITE #1,FIL$,NAM$,DAT$,XDCR$,DIA,FREQ$,DIST,STP,NSTEPS
1730 WRITE #1,RCVR$,MSK$,FOCUS$,COMMENT$
1740 INPUT "DIRECTION (+ OR -)";DIR$
1750 IF DIR$<>"+" AND DIR$<>"-" THEN 1740
1760 CMD$=DIR$
1770 GOSUB 2210
1780 CMD$="N"+STR$(ABS(CINT(STP*SCALE)))
1790 GOSUB 2210
1800 PRINT "RATE (1-";R$;")";
1810 INPUT RAT
1820 IF RAT=0 THEN 1850
1830 CMD$="R"+STR$(ABS(CINT(RAT)))
1840 GOSUB 2210
1850 PRINT "Hit RETURN when ready to scan, or any key then return to abort";
1860 INPUT "",YN$
1870 IF YN$="" THEN GOTO 1920
1880 CLOSE
1890 KILL FIL$
1900 RESET
1910 GOTO 2130
1920 CMD$="G"
1930 REM Read data, this section can either read from terminal or A/D board
1940 PRINT CLR$;"Type voltage readings in response to prompts."
1950 PRINT
1960 FOR I=0 TO NSTEPS-1
1970 PRINT "Data at point ";I;"=";
1980 INPUT "",VOLTS
```

```
1990 IF VOLTS=0 THEN PRINT "Error, zero input not allowed, repeat":GOTO 1970
2000 PRINT #1,VOLTS;",";
2010 IF I=NSTEPS-1 THEN 2030
2020 GOSUB 2210
2030 NEXT I
2040 IF DIR$="+" THEN CMD$="-" ELSE CMD$="+"
2050 GOSUB 2210
2060 CMD$="R "+R$
2070 GOSUB 2210
2080 CMD$="N"+STR$((NSTEPS-1)*ABS(CINT(STP*SCALE)))+C$+"G"
2090 GOSUB 2210
2100 PRINT #1,-1
2110 CLOSE
2120 RESET
2130 PRINT CLR$
2140 INPUT "RELEASE MOTOR";YN$
2150 IF MID$(YN$,1,1)="Y" THEN CMD$="I" : GOSUB 2210
2160 PRINT "SCAN COMPLETE"
2170 PRINT
2180 END
2190 REM
2200 REM Subroutine ot ouput string CMD$ to X motor controller
2210 FOR J=1 TO LEN(CMD$)
2220 CHAR=ASC(MID$(CMD$,J,1))
2230 GOSUB 2310
2240 NEXT J
2250 CHAR=13
2260 GOSUB 2310
2270 RETURN
2280 REM
2290 REM Subroutine to do I/O to X motor controller
2300 REM
2310 RETURN
2320 IF (INP(238) AND 1)=1 THEN 2320
2330 OUT 238, &HF1
2340 IF (INP(238) AND 1)=0 THEN 2340
2350 RETURN
```

B.3 WRTAPHP PROGRAM

```
10 REM ******************************************************
20 REM
30 REM   WRTAPHP  :  TRANSFERS DATA FILE TO HP TAPE
40 REM
50 REM  TRANSFERS FILE CREATED BY SCANX.BAS TO HP2647 LEFT
60 REM   DATA TAPE DRIVE.  DATA TAPE CAN THEN BE USED IN
70 REM   HP BASIC OR LOADED TO CMS VIA CMS COMMAND RDTAPHP.
80 REM
90 REM    BY JOHN GRAY    APRIL 1983
100 REM
110 REM ******************************************************
120 REM
130 REM  TO USE, PLUG HP TERMINAL INTO CCS 2200 FRONT PANEL PORT
140 REM  (PRINTER PORT) AND RUN THIS PROGRAM.
150 REM
160 REM
170 CLR$=CHR$(27)+H+CHR$(27)+J
180 PRINT CLR$;
190 PRINT "Plug HP2647 into front panel port on CCS 2200."
200 PRINT "Set terminal for 1200 baud, no parity, remote switch down."
210 PRINT "Place SCRATCH or other dummy tape into LEFT drive."
220 PRINT "Hit HP terminal reset switch twice."
230 INPUT "Press RETURN when ready.", A$
240 PRINT CLR$;
250 PRINT "Enter the full name of file to be transferred"
260 INPUT "to the HP data tape.";FIL$
270 REM TEST IF FILE EXISTS BEFORE TRANSFER
280 ON ERROR GOTO 610
290 OPEN 1,#1,FIL$
300 ON ERROR GOTO 690
310 INPUT #1,FIL$,NAM$,DAT$,XDCR$,DIA,FREQ$,DIST,STP,NSTEPS
320 INPUT #1,RCVR$,MSK$,FOCUS$,COMMENT$
330 ON ERROR GOTO 0
340 REM REWIND LEFT TAPE
350 LPRINT CHR$(27);",cRE L"
360 REM WRITE EACH DATA ITEM SEPARATELY
370 D$=FIL$ : GOSUB 770
380 D$=NAM$ : GOSUB 770
390 D$=DAT$ : GOSUB 770
400 D$=XDCR$ : GOSUB 770
410 D=DIA : GOSUB 810
420 D$=FREQ$ : GOSUB 770
430 D=DIST : GOSUB 810
440 D=STP : GOSUB 810
450 D=NSTEPS : GOSUB 810
460 D$=RCVR$ : GOSUB 770
470 D$=MSK$ : GOSUB 770
480 D$=FOCUS$ : GOSUB 770
```

```
490 D$=COMMENT$ : GOSUB 770
500 REM NOW TRANSFER NUMERICAL DATA
510 FOR I=1 TO NSTEPS+1
520 INPUT#1,D
530 GOSUB 810
540 NEXT I
550 IF D<>-1 THEN 690
560 LPRINT CHR$(27);",cRE L"
570 CLOSE #1
580 PRINT "transfer complete"
590 END
600 REM TEST IF FILE ERROR, ELSE USE SYSTEM ERROR MESSAGE
610 IF ERR=53 THEN 630
620 ON ERROR GOTO 0
630 CLOSE
640 PRINT
650 PRINT "Error, file ";FIL$;" does not exist. Try again."
660 PRINT
670 RESUME 250
680 REM FORMAT ERROR
690 PRINT CHR$(7);"ERROR: Data file not in proper format if created by"
700 PRINT "SCAN programs. Must have proper header format and end with"
710 PRINT "-1 as last data value. Use XFER to transfer general purpose"
720 PRINT "ASCII and data files."
730 PRINT "FILE NOT TRANSFERED!"
740 CLOSE
750 END
760 REM STRING TRANSFER ROUTINE
770 LPRINT CHR$(27);",cC L DA L";CHR$(13);
780 LPRINT D$
790 RETURN
800 REM NUMERIC DATA TRANSFER ROUTINE
810 LPRINT CHR$(27);",cC L DA L";CHR$(13);
820 LPRINT D
830 RETURN
```

REFERENCES

1. K. F. Graff, "A history of ultrasonics," in Physical Acoustics, 15, W. P. Mason and R. N. Thurston, eds., Academic Press (New York), 1979.

2. A. Macovski, "Theory on imaging with arrays," in Acoustic Imaging, G. Wade, ed., Plenum Press (New York), 1976.

3. J. D. Meindl, "Integrated electronics for acoustic imaging arrays," in Acoustic Imaging, G. Wade, ed., Plenum Press (New York), 1976.

4. G. D. Dockery, "Ultrasonic fields in fluids: Theoretical prediction using difference equations and three dimensional measurement using optical techniques," M.S. Thesis, Virginia Polytechnic Institute and State University, May 1983.

5. R. O. Claus, "EE6100 Advanced topics in electromagnetics: Applied ultrasonics," lectures, March 1983.

6. L. Filipczynski and J. Etienne, "Theoretical study and experiments on spherical focusing transducers with Gaussian surface velocity distribution," Acustica 28, 121 (1973).

7. F. D. Martin and M. A. Breazeale, "A simple way to eliminate diffraction lobes emitted by ultrasonic transducers," J. Acoust. Soc. Am. 49, 1668 (1971).

8. P. S. Zerwekh, "Design, construction, and testing of ultrasonic transducers with modified radial velocity profiles," M.S. Thesis, Virginia Polytechnic Institute and State University, March, 1982.

9. R. A. Burrier, personal communications, October 1982.

10. J. W. Gray, "Schlieren techniques and their application in viewing Schoch displacements," interim report for NASA grant NAG-1-192, "Acoustooptical techniques in ultrasonic transducer calibration for materials inspection," April 1982.

11. M. A. Breazeale, F. D. Martin, and B. Blackburn, "Reply to 'Radiation pattern of partially electroded piezoelectric transducers,'" J. Acoust. Soc. Am. 70, 1791 (1981).

12. B. P. Hildebrand, 'An analysis of pulsed ultrasonic arrays,' in Acoustical Holography VIII, A. F. Metherell, ed., Plenum Press (New York), 1980.

13. J. C. Wade, "Acoustooptical techniques for ultrasonic materials evaluation: Optical fiber interferometry and pulse echo systems," M.S. Thesis, Virginia Polytechnic Institute and State University, May, 1982.

BIBLIOGRAPHY

B. A. Auld, Acoustic Fields and Waves in Solids, Wiley 1973.

M. A. Breazeale, F. D. Martin, and B. Blackburn, "Reply to 'Radiation pattern of partially electroded piezoelectric transducers,'" J. Acoust. Soc. Am. 70, 1791 (1981).

R. A. Burrier, personal communications, October, 1982.

R. O. Claus and P. S. Zerwekh, "Three-dimensional far field measurements of a Gaussian profile ultrasonic transducer," Acoust. Soc. Am. National Meeting (Chicago, IL), April 1982.

R. O. Claus and P. S. Zerwekh, "Ultrasonic transducer with a two-dimensional Gaussian field profile," IEEE Trans. Son. Ultrason., 30, (1983).

R. O. Claus, "EE6100 Advanced topics in electromagnetics: Applied ultrasonics," lectures, March 1983.

D. R. Dietz, "Apodized conical focusing for ultrasound imaging", IEEE Trans. Son. Ultrason. SU-29, 128 (1982).

G. D. Dockery and R. O. Claus, "Difference equation technique for determining the evolution of radially symmetric ultrasonic fields," Proceedings of the Souteastern Conference of IEEE, p. 511, April 1983.

G. D. Dockery, "Ultrasonic fields in fluids: Theoretical prediction using difference equations and three dimensional measurement using optical techniques," M.S. Thesis, Virginia Polytechnic Institute and State University, May 1983.

P. D. Edwards, ed., Methods of Experimental Physics, Vol. 19: Ultrasonics Academic Press (New York) 1981.

L. Filipczynski and J. Etienne, "Theoretical study and experiments on spherical focusing transducers with Gaussian surface velocity distribution," Acustica 28, 121 (1973).

A. O. Garg, "Application of optical fibers to wideband differential interferometry and measurements of pulsed waves in liquids," Dept. of Elect. Eng., VPI & SU, Masters Thesis, July 1982.

K. F. Graff, "A history of ultrasonics," in Physical Acoustics, 15, W. P. Mason and R. N. Thurston, eds., Academic Press (New York), 1979.

J. W. Gray, "Schlieren techniques and their application in viewing Schoch displacements," interim report for NASA grant NAG-1-192, "Acoustooptical techniques in ultrasonic transducer calibration for materials inspection," April 1982.

J. W. Gray and R. O. Claus, "Variable amplitude, phase, and field shape ultrasonic transducers," Proceedings of the Souteastern Conference of IEEE, p. 416, April 1983.

B. P. Hildebrand, 'An analysis of pulsed ultrasonic arrays,' in Acoustical Holography VIII, A. F. Metherell, ed., Plenum Press (New York), 1980.

Y. A. Kondrat'ev, 'Pulsed operation of a focusing piezoelectric transducer,' Soviet J. of Nondestructive Testing 14, 688 (1978).

A. Macovski, "Theory on imaging with arrays," in Acoustic Imaging, G. Wade, ed., Plenum Press (New York), 1976.

F. D. Martin and M. A. Breazeale, "A simple way to eliminate diffraction lobes emitted by ultrasonic transducers," J. Acoust. Soc. Am. 49, 1668 (1971).

W. P. Mason and R. N. Thurston, eds., Physical Acoustics, 10, 14, 15, 16, Academic Press (New York), 1979.

J. D. Meindl, "Integrated electronics for acoustic imaging arrays," in Acoustic Imaging, G. Wade, ed., Plenum Press (New York), 1976.

H. T. O'Neil, "Theory of focusing ultrasonic radiators," J. Acoust. Soc. Am. 21, 360 (1949).

W. Sachse and N. N. Hsu," Ultrasonic transducers for materials testing and their characterization", in Physical Acoustics, 14, W. P. Mason and R. N. Thurston, eds., Academic Press (New York), 1979.

A. D. Vopilkin, et. al. 'Wide-band ultrasonic transducer and its uses,' United States Patent 3968680, July 1976.

G. Wade, ed., Acoustic Imaging, Plenum Press (New York), 1976.

J. C. Wade, "Acoustooptical techniques for ultrasonic materials evaluation: Optical fiber interferometry and pulse echo systems," M.S. Thesis, Virginia Polytechnic Institute and State University, May, 1982.

G. W. Willard, 'Focusing ultrasonic radiators,' J. Acoust. Soc. Am., 21, 360 (1949).

P. S. Zerwekh, "Design construction and testing of ultrasonic transducers with modified radial velocity profiles," M.S. Thesis, Virginia Polytechnic Institute and State University, March, 1982.

P. S. Zerwekh and R. O. Claus, 'An ultrasonic transducer with Gaussian radial velocity distribution,' IEEE Ultrasonics Sym. 2, 974 (1981).

The vita has been removed from the scanned document